

6-12-2014

# Global summation of radial frequency patterns and the effect of sudden onset glare on shape discrimination

Edgar Ekure  
*Nova Southeastern University*

This document is a product of extensive research conducted at the Nova Southeastern University [College of Optometry](#). For more information on research and degree programs at the NSU College of Optometry, please [click here](#).

Follow this and additional works at: [https://nsuworks.nova.edu/hpd\\_opt\\_stuetd](https://nsuworks.nova.edu/hpd_opt_stuetd)

 Part of the [Optometry Commons](#)

All rights reserved. This publication is intended for use solely by faculty, students, and staff of Nova Southeastern University. No part of this publication may be reproduced, distributed, or transmitted in any form or by any means, now known or later developed, including but not limited to photocopying, recording, or other electronic or mechanical methods, without the prior written permission of the author or the publisher.

---

## NSUWorks Citation

Edgar Ekure. 2014. *Global summation of radial frequency patterns and the effect of sudden onset glare on shape discrimination*. Master's thesis. Nova Southeastern University. Retrieved from NSUWorks, College of Optometry. (10)  
[https://nsuworks.nova.edu/hpd\\_opt\\_stuetd/10](https://nsuworks.nova.edu/hpd_opt_stuetd/10).

This Thesis is brought to you by the College of Optometry at NSUWorks. It has been accepted for inclusion in College of Optometry Student Theses, Dissertations and Capstones by an authorized administrator of NSUWorks. For more information, please contact [nsuworks@nova.edu](mailto:nsuworks@nova.edu).

**Global summation of radial frequency patterns and the effect  
of sudden onset glare on shape discrimination**

**By**

**Edgar U Ekure**

**Submitted to the Clinical Vision Research Program, College of  
Optometry of Nova Southeastern University in partial fulfillment of  
the requirements for the degree of**

**Master of Science**

**2014**

**Global summation of radial frequency patterns and the effect  
of sudden onset glare on shape discrimination**

**By**

**Edgar U Ekure**


**Approved as to style and content by:**



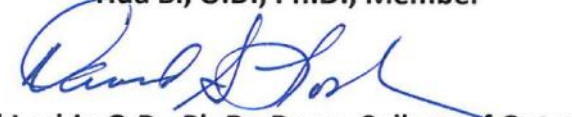
**Bin Zhang, M.D., Ph.D., Chair**



**Josephine Shallo-Hoffmann, Ph.D. F.A.A.O., Member**



**Hua Bi, O.D., Ph.D., Member**



**David Loshin O.D., Ph.D., Dean, College of Optometry**

## **Dedication**

**This Thesis is dedicated to all researchers who work tirelessly to advance our understanding of the complexities of the neural bases of visual perception**

## **Acknowledgement**

**Special thanks goes to my thesis advisor, Dr. Zhang, for the incredible mentorship he gave me; for sparking my interest in various aspects of visual perception and for guiding me through every aspect of this research work, without which this study would have been impossible.**

**I also want to acknowledge the contribution of others like BinBin Su, Rusa, Chuan Hu, and Jiang for their help in data collection. I must also specially thank Dr. Bi for her painstaking corrections, trimming of all rough edges and other indelible advice.**

**I would like to thank Professor Shallohoffmann for her overall support throughout the program, for promptly responding to various concerns and being ready to give strong recommendations when needed.**

**I also want to thank Patrick Hardigan for teaching me how to analyze statistical data.**

**I feel adequately prepared to be part of any clinical research endeavor having completed the Clinical Vision Research program for which I thank all the members of faculty.**

## **ABSTRACT**

### **Global summation of radial frequency patterns and the effect of sudden onset glare on shape discrimination**

The purpose of this study was to provide evidence of global pooling around the circumference of the Radial frequency (RF) pattern, and to study the effect of sudden onset glare on shape discrimination. The RF stimuli were generated by the amplitude modulation of the radius of a circle which deforms them from circularity, while the cross sectional luminance profile was the fourth derivative of Gaussians (D4). The amplitude of the stimuli determines how distinct the pattern is and thus measures the degree of sensitivity while the radial frequency determines the number of lobes the pattern has. In the first part of the study, whole RF patterns (RF3 to RF16) and open component fractions (0.125, 0.25, 0.5, 0.75), which are incomplete sectors of the whole, were tested against their respective reference unmodulated patterns. Subjects were tasked with discriminating minute deviations from their reference patterns. In the second part of the study, high contrast (20 X detection threshold) RF3 and RF4 contours and equivalent low contrast (5 X detection threshold) RF3 and RF4 contours were used as stimuli. Shape discrimination threshold for the high contrast target was determined with and without sudden onset glare. The result of the first part of the study showed that threshold decreased significantly as larger component RF patterns were tested ( $p < 0.05$ ). The decrease could not be accounted for by the probabilistic sampling of local filters (probability summation). The result of the second part of the study showed that shape discrimination threshold increased with sudden onset glare. The increase was even more pronounced with lower mean luminance and when smaller fractions of the contours were tested. Shape discrimination threshold was significantly higher with high contrast contours in the presence of glare than equivalent low contrast contours, indicating that the veiling luminance model alone could not account for a decrease in visual performance in this shape discrimination task.

ACKNOWLEDGEMENTS	iv
ABSTRACT	v
TABLE OF CONTENTS	vi
LIST OF FIGURES	vii
PART ONE	
INTRODUCTION: GLOBAL SUMMATION OF RADIAL FREQUENCY PATTERNS	1
METHODS	10
RESULTS	16
DISCUSSION	24
CONCLUSION	27
PART TWO	
INTRODUCTION: EFFECT OF SUDDEN ONSET GLARE ON SHAPE DISCRIMINATION	28
METHODS	31
RESULTS	38
DISCUSSION	43
CONCLUSION	46
BIBLIOGRAPHY	47
APPENDIX A-O: RAW DATA	54-68

## LIST OF FIGURES

### PART ONE

FIGURE 1: RADIAL FREQUENCY PATTERNS	12
FIGURE 2: RF PATTERNS WITH DIFFERENT COMPONENT FRACTIONS AND CONTRAST	15
FIGURE 3: PLOT OF RADIAL AMPLITUDE MODULATION VS. COMPONENTS	20
FIGURE 4: PLOT OF WHOLE RF4 AND RF8	21
FIGURE 5: PLOT OF RADIAL MODULATION VS. COMPONENTS AT LOW CONTRAST	23

### PART TWO

FIGURE 6: SCHEMATIC REPRESENTATION OF THE GLARE EXPERIMENTS	33
FIGURE 7: PICTURES OF RF CONTOUR AND GLARE SOURCE	36
FIGURE 8: PLOT OF THRESHOLD POINTS WITH AND WITHOUT GLARE	41
FIGURE 9: PLOT OF THRESHOL POINTS FOR PARTIAL RF CONTOURS	42



## **PART ONE**

### **CHAPTER ONE**

#### **GLOBAL SUMMATION OF RADIAL FREQUENCY PATTERNS**

##### **INTRODUCTION**

The quest to understand visual perception is probably as old as humans, however the earliest documented evidence of this quest dates back to the pre-Socratic era (Zemplen, 2005; Adamson, 2006; Pastore, 1971; Grusser, 1986). Broadly the major philosophical schools of thought in visual perception were the intromission and extromission schools. Intromissionists held the view that “emanations” from an object entering the eye cause visual perception, while extromissionists claim the opposite. Philosophers like Empedocles probably held both views since he alludes to the eye shooting fire like a lantern, while at the same time believing that the eye contains pores that serve as receptacles that must exactly fit the emanations from the object for perception to occur (Zemplen, 2005; Grusser, 1986; Adamson, 2006; Wade, 1999). A fully morphed hybrid of the two schools of thought was established in the era of Plato, who believed that visual perception occurs with a coalescence of the internal and external fires outside the body. The first quasi-advanced theory at that time was propounded by Aristotle, who did not buy into the intromission and especially extromission theories because as he correctly asserts, if perception comes by rays emanating from the eye then one should be able to see clearly at any given time, even in complete darkness (Zemplen, 2005). These primeval theories of vision persisted through the middle ages and not much was done to advance scientific thought in that historical epoch. It was not until the 16<sup>th</sup> and 17<sup>th</sup> Century that the basis of modern ideas of vision perception began to take root with the work of Johannes Kepler

(1571-1630) who argued that intromitted rays were refocused by the Crystalline lens unto the retina where perception is made possible (Schmolesky, Webvision).

The most basic understanding of the anatomy of the Eye and Central Nervous System (CNS) that were stunted largely as a result of religious prohibitions on dissection of human corpses prevalent in the Middle Ages began to emerge between 1600-1860 AD (Schmolesky, Webvision; Pastore, 1971; Smith, 1990). During this period the connection between the optic nerve to the Lateral Geniculate body after decussating at the chiasm, and the projection to the Cortex were known. Significant advances in histology with the discovery of the light microscope led to the discovery of the neuron as the basic unit of the CNS; the scientist with the greatest contribution to our modern knowledge of the neuron is none other than Santiago Ramon y Caja (1852-1934). Further development and the discovery of the neuronal synaptic junction came with the discovery of the electron microscope (Schmolesky, Webvision).

It was the pioneering work of Hubel and Wiesel (1962, 1965, 1968) that gives us the first clear insight into understanding the early stages of form processing at the V1 level. They demonstrated that the striate cortex is made up of three types of cells: simple, complex and hyper-complex cells. Simple cell receptive fields are thought to be built from the more circular center- surround pattern of RGC and LGN receptive fields; but simple cell receptive fields are more elongated in shape with an active excitatory zone which may be flanked by inhibitory zones on both sides. These cells respond optimally to line stimuli of appropriate widths and orientations.

Complex cells on the other hand, although having receptive field with the same spatial configuration as simple cells, respond only to dynamic line stimuli; static stimuli elicit virtually no response. Here we see early evidence of motion processing in the visual system (Albus and Fries, 1980; Blakemore and Tobin, 1972; Bolz and Gilbert, 1986; Born and Tootell, 1991; DeValois et al., 1985; Dreher, 1972; Fries et al., 1977; Hubel and Wiesel, 1965; Kato et al., 1978; Maffei and Fiorentini, 1976; Nelson and Frost, 1978; Orban et al., 1979a, b; Rose, 1977; Sillito, 1977; Sillito and Versiani, 1977; Tanaka et al., 1987; von der Heydt et al., 1992; Yamane et al., 1985).

Hubel and Wiesel, (1965) initially classified hyper-complex cells as distinct cellular types based on their end-stopping behavior. Subsequent studies (Dreher, 1972; Gilbert, 1977; Kato et al., 1978; Rose, 1977) have demonstrated this behavior in simple and complex cells; therefore hyper-complex cells are now considered subsets of simple and complex cells. End-stopped cells respond maximally to lines with properly defined length, width and orientation and therefore will respond to angles and edges. This forms the basis of our current understanding of the early stages of local contour processing (Loffler, 2003). We now know that at this stage filters respond maximally to local aspects of a stimulus that are finely tuned to their spatial frequency, orientation and phase dimensions (Loffler, 2008; De Valois et al., 1982; Hubel and Wiesel, 1968; Heeger, 1992; Wilson & Humanski, 1993; Bonds, 1989; Bonds, 1991; Das and Gilbert, 1999; Das and Gilbert, 1995).

Having demonstrated that early V1 neurons respond only to discrete or local aspects of an object, the self-evident question becomes why and how do we see an unbroken, whole visual percept of that object in space? Many studies have demonstrated that neurons make both

proximal and distal connections with their neighbors which have led some to argue that these local connections alone are sufficient to account for the global perception of an object in space. Psychophysically the existence of these neuronal connections has been shown through the phenomenon of contour interaction. Polat and Sagi, (1993, 1994), showed the phenomenon of contour interaction through collinear facilitation by demonstrating that the threshold for the detection of a Gabor stimulus is elevated when flanked by a supra-threshold Gabor with a separating distance of less than  $2\lambda$ . On the other hand however, threshold of the Gabor target decreases with increasing target-flanker separation up to  $2-3\lambda$ , beyond which it begins to increase again. This shows that shorter ( $< 2\lambda$ ) target-flanker separation induces spatial suppression or masking, while longer target-flanker separation induces facilitation. It is important to note that maximum facilitation is induced when target and flanker have the same orientation, the axis of orientation aligns vertically rather than horizontally (iso-orientation), and spatial frequency of target and flanker is low. The phenomenon of collinear facilitation thus makes it especially tempting to conclude that perception of a spatially extensive object might be made possible by the integration of the local responses of V1 neurons, since all the information are present at this stage. However if this were the case, it will undoubtedly lead to a massive information glut and the attendant computational difficulty of segregating fore-and back-ground information. To account for the visual system's ability to discriminate fore-ground from back-ground without linkage, a hierarchical model was developed. The literature provides compelling evidence of this hierarchical strategy (Habak et al., 2004; Van Essen et al., 1992) where output signals from lower stages V1 and V2 feed into higher centers V4 and V3/VP in the ventral processing stream, for intermediate stages of form processing (Goodale and Milner,

1992). Further evidence from neurophysiological studies (Gallant et al., 1993; Parsupathy & Connor, 2001, 2001; Dumoulin and Hess, 2007) have demonstrated that area V4 responds maximally to non-Cartesian shapes like circles, concentric circles and ellipses; and Gallant et al., (2000) showed that a clear deficit in shape discrimination existed in a patient with a lesion in V4.

Other higher cortical centers involved in shape processing include: the infero-temporal (IT) cortex, which is the highest level of the ventral stream; the Fusiform Face area (FFA), neurons of which have been shown to respond to complex forms like faces; Parahippocampal place area (PPA) and Lateral occipital cortex (LOC) (Brincat and Connor, 2004; Desimone, 1991; Gross, 1992; Tanaka, 1996; Young, 1992). Neurons from IT (Kayaert et al., 2003; Brincat and Connor, 2004) and FFA (Valentine, 1991; Loffler et al., 2005) seem to code information for a proto-typical shape and that of the human face. Neuronal firings in the afore-mentioned areas have been shown to increase with distance of a stimulus from this proto-typical shape or face.

The hierarchical model thus demonstrates that early parts of the striate cortex, V1, V2 respond to edges and angles, the intermediate stages V3, V4 respond maximally to more global aspects of an image especially non-Cartesian shapes while higher centers like the FFA respond to complex shapes like faces. This study aims to demonstrate the existence of the intermediate stages of shape processing by showing global pooling around non-Cartesian stimuli, using visual psychophysical paradigms. The logic here is that if a different mechanism is involved in discriminating local and global aspects of shapes, performance in both tasks will be different. Furthermore, if there is a higher processing stage other than V1 in processing global shape,

then performance in a global task should be better than that of the local aspects of the given task.

Psychophysical studies using radial frequency (RF) stimuli to form non-Cartesian patterns have been used to study global shape processing (Wilkinson et al., 1998; Loffler, 2008; Bell and Kingdom, 2009; Bell et al., 2007; 2009; 2010; Schmidtman et al. 2012; Mullen and Beaudot, 2002; Mullen et al., 2011). The suitability of the RF stimulus for psychophysical studies is because it lends itself easily to parametric manipulation. The RF pattern is formed by the amplitude modulation of the radius of a circle with the function below:

$$R(\Theta) = r_0[1 + A\sin(\omega\Theta + \Phi)] \text{-----}(1)$$

A is the radial modulation amplitude,  $\omega$  is the radial frequency,  $\Phi$  is the angular phase. The radial amplitude modulation (A), determines how distinct the pattern is; the radial frequency ( $\omega$ ), determines the number of lobes the pattern has; and the phase angle ( $\Phi$ ), determines the orientation of the pattern (Figure 1). The function  $R(\Theta)$  generates a perfect (unmodulated) circle when amplitude is set at zero.

Several studies (Wilkinson et al., 1998; Loffler, 2008; Bell and Kingdom, 2009; Bell et al., 2007; 2009; 2010; Schmidtman et al., 2012) have reported increased performance (decrease threshold) with RF patterns as the number of lobes increases to between 8-10/360°, beyond which threshold begins to increase (performance decreases), indicating that a global mechanism summing responses around the circumference of the pattern is clearly in play, otherwise one would logically expect to find no significant change in performance level between RF1 or RF5 or more if the process was mediated solely by locally oriented filters.

Another way to put it is that if a global shape mechanism operating at an intermediate level is involved in the processing of RF patterns, performance on the whole RF pattern will be better than the sum of its parts (Bell et al., 2010).

Wilkinson et al., (1998) studied the detection and recognition of radial frequency patterns through a series of experiments. First, they measured basic threshold detection from circularity using RF pattern with a mean radius of  $0.5^\circ$ , spatial frequency of 8 cpd and amplitude modulation varying logarithmically at different radial frequencies. Threshold declined (performance improved) almost 2 log units from a high at RF1 to an asymptote around RF3 to RF5. The result showed that the detection of RF patterns in human is in the hyperacuity range because it ranged from 2-9" when the amplitude of minimum distortion is expressed in seconds of arc. The Amplitude of minimum distortion expressed as a proportion of the radius of the circle yields a fraction known as the Weber fraction; the average Weber fraction in their study was 0.003. Their third experiment was on radial frequency identification. Subjects were presented with supra-threshold patterns having different radial frequencies, which were presented within a short interval (167 ms). For radial frequency between 3-6 cycles/ $360^\circ$ , median performance was above 90% correct; for RF above 8 cycles/ $360^\circ$ , performance fell dramatically. Wilkinson et al. explained their results by positing that global pooling of local contour signals around the circumference of the circle occurs and that the limitation of this global mechanism at higher RF is the reason for the shortfall in performance.

If a global mechanism is in play with RF patterns, one will expect that the performance of the whole pattern will be better than its parts. To address this concern, Wilkinson et al., 1998 in their second experiment compared performance with sinusoidally modulated straight lines with

that of the closed RF pattern. The base stimuli of the lines had the same luminance profile and spatial frequency as that of the circle; the distance separating the two lines was also equivalent to the diameter of the circle. The results showed that performance was better for the closed RF contour at lower contrast than at 100% contrast at which point they were identical. These results pose a serious challenge to models that negate the importance of a global mechanism but instead postulate that local inter and intra-filter interactions at early parts of the visual pathway (V1) are enough to explain the perception of smooth contours.

More recently Bell et al., 2010, further demonstrated evidence of global mechanism in RF patterns at supra-threshold levels, by using radial frequency amplitude adaptation effects (RFAAE). The rationale for using RFAAE is based upon the fact that adaptation to RF patterns of known amplitudes shifts the perceived radial amplitude modulation of a test RF pattern in a direction away from that of the adaptor. The adaptation effect was measured as the additional modulation amplitude required to make the test probe and the reference probe appear the same; this, they called the point of subjective equality (PSE). It is reasonable to assume that if the PSE is greater for the whole RF pattern than for its parts, then a global mechanism could be involved in the processing of the whole RF pattern. Their first experiment was a comparison of the size of the RFAAE of the test RF pattern after adaptation with the whole versus parts of the adaptor RF pattern. The result demonstrated that after adaptation to the “whole” adaptor stimulus field, subjects required an average of 12% more amplitude of modulation to reach PSE with the reference probe. With the probe stimuli comprised of the parts of the pattern, no observer showed a significant positive shift in the PSE. It is therefore reasonable to conclude that the after-effect in the whole pattern probe was specific to the global form of the stimulus.



This notion is however not a consensus, Mullen et al., 2011 for example, found no significant difference in threshold when performance with whole RF patterns were compared to their component parts. Clear differences in the methodology could account for the discrepancy in the results demonstrated by Mullen et al., 2011 and that of others (Wilkinson, 1998; Loffler, 2003; Dickinson et al., 2012; Schmidtman et al., 2012). It will be noteworthy to mention that the stimuli used by Mullen were contrast scaled at 5 times detection threshold and also presented in the cosine phase instead of sine phase as used by others.

We provide, in this study, further evidence of a global pooling around the RF contour using two experiments. RF patterns with radial frequencies between 3-16 cycles/360<sup>o</sup> were used. Threshold was determined as the minimum percentage radial amplitude modulation required to just perceive the test patterns as different from various reference patterns. Performance of the whole pattern was compared to that of component parts of the RF patterns. Stimuli for Experiment 1 were high contrast (100%) RF contours, while that of experiment 2 were contrast scaled at 5 times detection threshold and presented in the sine phase.

## CHAPTER TWO

### METHODS

#### Apparatus

All stimuli were generated using Matlab 2010b (Mathworks) and Psychtoolbox (Bernard, 1997; Peli, 1997). The host computer was Windows 7 based PC (Dell Optiplex, 780). All stimuli are displayed on a gamma corrected CRT monitor (Richard Electronics, 15.3" W X 11.5" H), with resolution of 1280 X 1024 and a refresh rate at 100 Hz. The luminance of the pattern was 50 cd/m<sup>2</sup> while contrast was linearized at 256 equally spaced grey levels. Subjects were seated 60 cm from the computer monitor in complete dim illumination with chin placed in the chin rest and forehead on the forehead rest to maintain a stable fixation distance. At this distance the stimuli covered an area of about 512 X 512 pixels.

#### Stimuli

The stimuli were radial amplitude modulation of the radius of a circle derived using equation (1)

$$R(\Theta) = r_0[1 + A\sin(\omega\Theta + \Phi)] \text{-----}(1)$$

A is the radial modulation amplitude,  $\omega$  is the radial frequency,  $\Phi$  is the angular phase, while  $\Theta$  represents the polar coordinates. The radial amplitude modulation (A), determines how distinct the pattern is; the radial frequency ( $\omega$ ), determines the number of lobes the pattern has; and the phase angle ( $\Phi$ ), determines the orientation of the pattern. The equation generates a perfect (unmodulated) circle when amplitude is set at zero (Figure 1a and 1b). The amplitude A was always set between 0 and 1 to prevent the crossing of the closed patterns; also the phase of the pattern was varied to ensure subjects were not able to predict the position of the lobes.

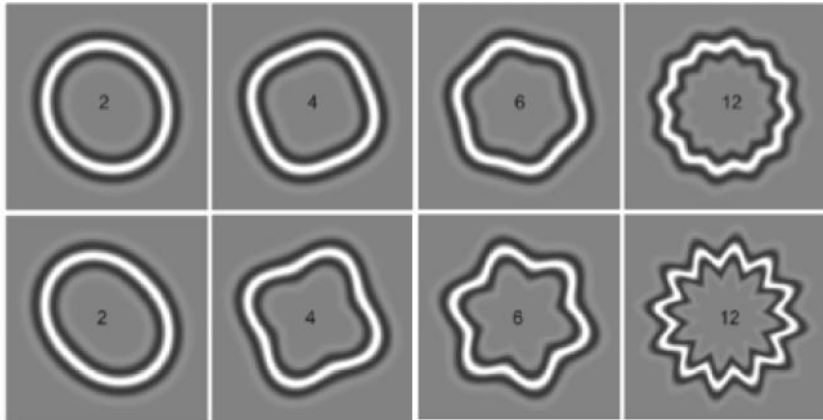
The cross-sectional luminance profile of the RF pattern used in this study is defined by the fourth derivative of Gaussians (D4) and represented by the equation 2 below:

$$D4(r) = C\{1 - 4[(r - r_0)/\sigma]^2 + (4/3)(r - r_0)/\sigma\}^4 \exp[-((r - r_0)/\sigma)^2] \text{-----}(2)$$

C is the contrast of the contour, r and  $r_0$  is the radius and mean radius respectively, while  $\sigma$  determines the peak spatial frequency which was set at 8 cpd for this study, full spatial frequency bandwidth at half amplitude was 1.24 octaves.

In the first experiment different fractions of open RF patterns were used at high contrast levels, here contrast was set at 100%. In the second experiment different fractions of RF patterns at low contrast levels (5 times detection threshold) were used (Figure 2). Fractions of RF patterns were created by restricting the radial frequency contour between specific polar angles.

(a)



(b)

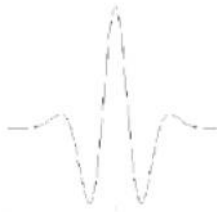
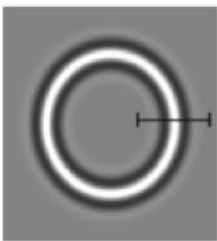


Figure 1. (a) Shows different RF patterns with increasing RF from left to right, while amplitude modulation of the lower row is higher than the top row. (b) Shows an unmodulated pattern with its cross-sectional luminance profile, which is defined by the 4<sup>th</sup> derivative of Gaussians, below.

## Experimental Protocol

The procedure used in this study was the temporal two-alternative forced choice (2AFC) paradigm. The reference and test contours were randomly presented to ensure the subjects could not predict the test pattern based on which one comes first. The time lapse between the presentation of the reference pattern and test pattern was 160ms and the inter-stimulus presentation time was 300 ms. The task of the subjects was to discriminate between modulated ( $A > 0$ ;  $A \leq 1$ ) and unmodulated ( $A = 0$ ) patterns. These six modulation amplitudes were used, 0.20, 0.3, 0.4, 0.5, 0.75, 1.0, with each amplitude tested 30 times, making a total of 180 presentations per experiment. The response criterion used was that the amplitude was decreased after two correct responses and increased after one wrong response. The responses of the subjects were automatically recorded when they pressed the left pointing arrow key on the computer key-board indicating that the first presentation was the modulated pattern or when they pressed the right pointing arrow key indicating that the second presentation was the modulated pattern. No feedback was given to the subjects.

The first part of the experiment was the basic threshold determination, which was then used to set the contrast levels of experiment 2; the high contrast experiment was set at 100% contrast while the low contrast experiment was set at 5 X detection threshold. To evaluate for the presence and strength of global summation, different fractions of RF3, 4, 6, 8, 10, 12 and 16 were modulated and compared with their respective reference patterns. For each amplitude modulation point, threshold was computed for 62.5% correct response using the maximum likelihood psychometric analysis and fitted with the Weibull model. Bootstrap analysis of 500

simulations indicated that the model was good fit. All targets were viewed binocularly and two practice sections were carried out.

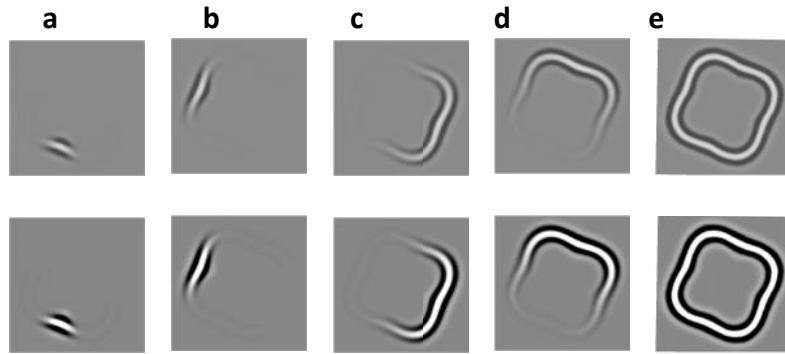


Figure 2. RF4 patterns with different fractions: a = 0.12 (12.25%), b = .25 (25%), c = 0.50 (50%), d = 0.75 (75%), e = 1.0 (100%). The top row consists of low contrast contours while the bottom row has the high contrast contours.

### **Subjects**

All subjects had normal or corrected to normal visual acuities and had neither ocular pathologies nor binocular vision anomalies. They all underwent 2 practice sections before the actual experiments.

### **Declaration**

The study was approved by the Nova Southeastern University Institutional review board (IRB) and done in accordance with the Helsinki declaration of the use of human subjects.

## **Experiment 1**

This experiment tested the hypothesis that performance with closed (whole) contour RF pattern is better than the sum of its open parts, which will logically prove the existence of a global mechanism summing local information around the circumference of the RF pattern. Stimuli were radial modulation of the radius of a circle (eq. 1), with a cross-sectional luminous profile given by the 4<sup>th</sup> derivative of Gaussians (D4). Different fractions of RF4, 6, 8, 10, 12 and 16 were generated by restricting the RF contours to various polar angles (Fig. 2). This first experiment was conducted using high contrast targets (Fig. 2 bottom row).

## **Experiment 2**

The same protocol and stimuli used in experiment 1 were also used in 2. The only fine detail is that whereas the stimulus contrast used in experiment 1 was high (100%), that of experiment 2 was low at 5 X detection threshold.

## CHAPTER THREE

### RESULTS

#### EXPERIMENT 1

Figure 3 shows data representation for four (4), out of eight (8) subjects of experiment 1, (100% contrast), while figure 3A shows the mean plot of all subjects. All data clearly demonstrate that threshold declined (performance increased) significantly as the percentage component parts of the RF pattern increased; a trend which was demonstrated for all subjects. For all the subjects, threshold was lowest for the whole RF pattern than for any of its component parts, on the other hand, threshold was highest for all RF pattern (RF3-RF16) at the least percentage component (12.5%) and declined rapidly to an asymptotic level around the 50% component.

Two factor analysis of variance (ANOVA) was performed. The first factor was the RF type with seven levels (3, 4, 6, 8, 10, 12 and 16), while the second factor was the component RF fractions modulated, and had five levels (12.5, 25, 50, 75 and 100%). There was statistically significant difference in the threshold amplitude modulation in the different RF type ( $p < 0.001$ ), there was also a significant decrease in threshold amplitude modulation as the proportion of RF pattern increased ( $p < 0.01$ ); interestingly there was significant interaction between the two factors ( $p < 0.01$ ). Taken together, threshold decreased with increasing radial frequency and also with increasing proportions of the RF patterns. This result both demonstrates the existence of a global mechanism summing responses around the circumference of the RF pattern and the strength of the summation. The interaction effect shows that both factors act together to influence the radial amplitude modulation pattern. ANOVA post hoc analyses (Tukey) showed a significant difference in all combinations of factor one with the weakest significance between



RF3 and RF4 ( $p = 0.043$ ); between RF3 and RF6 ( $p < 0.01$ ), RF3 and RF12 was  $p < 0.01$ ). Post hoc analyses of the component fractions did not reveal any significant difference between 12.5 and 25% of the component part ( $p > 0.05$ ) but there was significant difference in threshold for all other combinations of the component parts. There was a strong negative correlation between threshold of the RF contour and the component fractions. Correlation between component parts of RF3 contour and their threshold was -0.766, RF4 (-0.815), RF6 (-0.734), RF8 (-0.677), RF10 (-0.606), RF12 (-0.60) and RF16 (-0.38). The mean correlation for all data was 0.404. The negative correlation indicates that threshold decreases as the proportion of the component parts increase. Overall data show a strong dependence of threshold on both the number of RF and the proportion of the pattern viewed by subjects.

If we take the ratio of threshold of the 0.125 component of the RF3 pattern to that of the whole, we will have 5.96 as the average ratio, and for individual subjects we will have ( $S1 = 7.5$ ;  $S2 = 8.5$ ;  $S3 = 6.09$  and  $S4 = 3.52$ ), such high ratios again are consistent with a very efficient global integration process (Dickinson et al. 2012).

Threshold decline with increasing proportion of the RF pattern has been demonstrated to be sharp in this study, but since a decline in threshold can reasonably be expected merely from a probabilistic summing of the responses of independent detectors from their inherent noisy signals, it is important to show that the decline seen in this study cannot be accounted for by this probability summation. The decrease in threshold from the 0.125 component of RF3 for subject S1 corresponds to a slope of -0.98, a far more efficient decrease than one will expect from probability summation which in this study was determined to be -0.48. For S2 it was -

1.013, -0.77 for S3 and -0.97 for S4. This same pattern of decline in the slope was observed for RF patterns up to RF8, beyond which there was a decline that could be accounted for by probability summation. All aforementioned subjects had less than -0.40 in the slope connecting the 0.125 component part to the whole for RF contours over RF10.

Global summation is assumed when performance on a task with global pattern is better than that of its component parts since local neural mechanisms code for local aspects of such patterns. The above results show further evidence of a global mechanism that mediates intermediate shape processing by demonstrating improved performance with whole RF patterns compared to the sum of its parts.

Mullen et al., (2011) asserted that information that limits threshold in the RF pattern is contained in their local components and showed in their study that threshold obtained for local components of the RF pattern was not significantly different from that of the whole. This implies that threshold is not set by a global shape processing mechanism but by the integration of local signals from local filters at earlier stages of shape processing. The reason they offered for the discrepancy with other studies was that those studies compared modulation of fractions of closed RF patterns to the modulation of the whole. They further opined that if progressively larger fractions were removed from an RF pattern, then performance with local fractions of open contours will be similar to that of whole closed ones. This implies that the unmodulated sectors of the closed contours were responsible for the difference in threshold. If this were so we should expect that threshold for closed contours with a local fraction modulated will be significantly lower than of a similarly modulated fraction of an open contour; although Mullen

et al., (2011) seem to imply that it may be responsible for the higher threshold seen in other studies contrary to their initial assertion. We addressed this by conducting a control experiment with two closed contours RF4 and RF8. Different fractions of these contours, similar to those already shown for open contours were modulated and threshold for both compared. Although threshold for the open contours were slightly higher, contrary to what should be expected, paired samples t-tests did not reveal any significant difference ( $p > 0.05$ ) for the four observers tested (Figures 4a-4d). Our data therefore does not support the claim that improved performance with closed contours is a result of the unmodulated sectors.

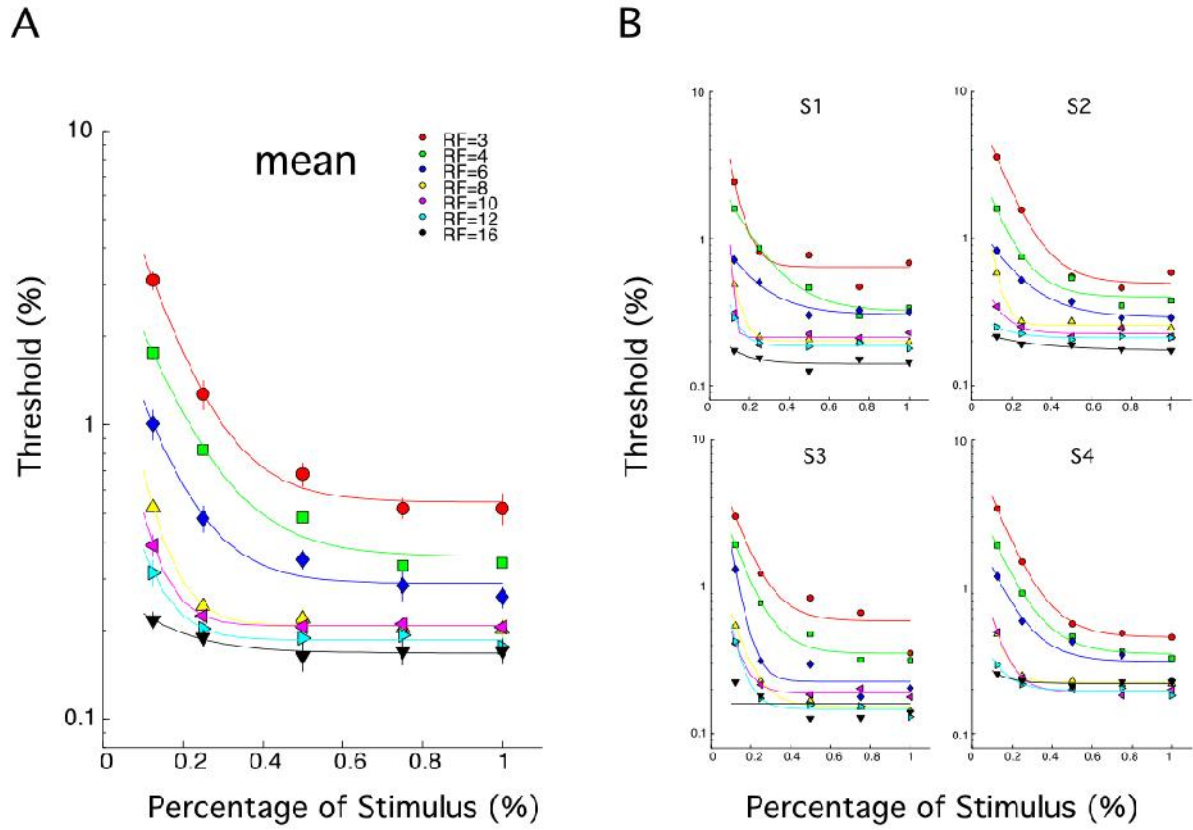


Figure 3: % radial amplitude modulation was plotted as a function of component fractions. Contrast was set at 100%. Different color points represent the various RF patterns, and as can be seen, % radial amplitude modulation declined with increasing component fractions.

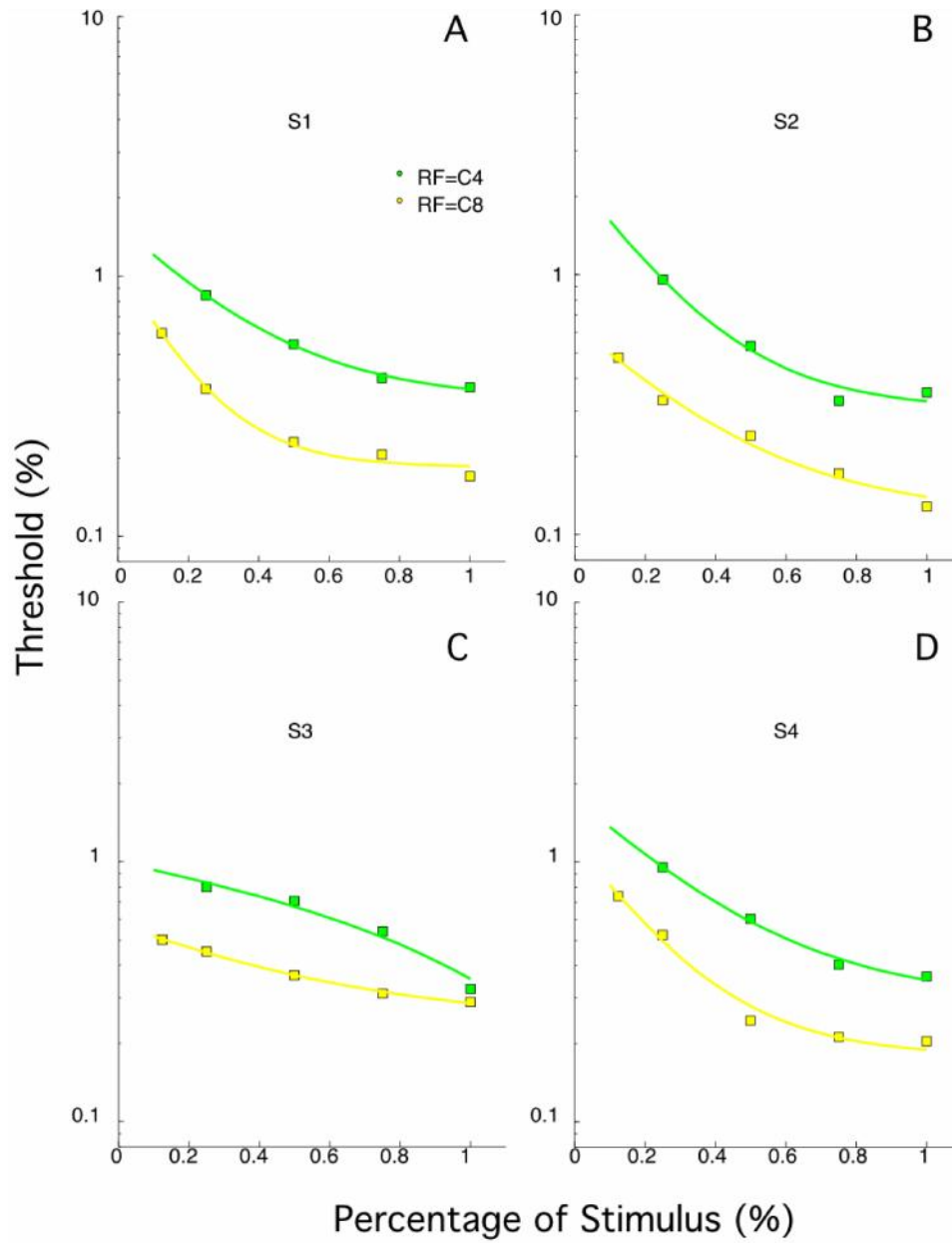


Figure 4: representative plots of % radial amplitude modulation vs. fractions of whole RF4 and RF8 contours. There was no significant difference ( $p < 0.05$ ) in threshold when similar modulated fractions of open contours were compared to that of closed contours.

## EXPERIMENT 2

The same protocol and stimuli used in experiment 1 were also used in 2. The only fine detail is that whereas the stimulus contrast used in experiment 1 was high (100%), that of experiment 2 was low at 5 X detection threshold (Figure 2 top row).

Results of experiment 2 are displayed below in figure 5; similar trends as seen with high contrast stimuli were also seen with contrast at 5 X detection threshold the only difference being that lower contrast increases threshold by about a factor of 2. Similar increase in threshold has been reported (Shmidtman et al., 2012). The reduction in sensitivity due to contrast was seen for all RF contours and local component fractions (0.125 and 0.25); however, as larger component fractions were tested, threshold approximated that seen when contrast was set at 100%. The initial increase in threshold with lower component fractions was more obvious with RF3 as can be seen from the data (Fig. 5a-5d). Although threshold increased with lower contrast set at 5 X detection threshold, there was a statistically significant decrease in threshold as larger component fractions were tested for all subjects. Two-factor ANOVA showed a significant decline in threshold with RF pattern and component fractions tested ( $p < 0.01$ ); there was also a significant interaction between the two factors ( $p = 0.0298$ ). The ratio of threshold of 0.125 component, to that of the whole for RF3 for the subject in Fig. 5(a) was 9.8/1 which is such a steep increase that it suggests an efficient global integration process. The same pattern was seen across subjects and for other RF patterns. Mullen, Beaudot and Ivanov, (2011) are contrarians with respect to the view that a global integration process sums information around the circumference of the RF patterns and determines threshold. Although they used RF

patterns set at 5 X detection threshold as was used in this study, our results did not replicate their findings, and thus we conclude in favor of a global mechanism active at intermediate stages of form processing as the reason for the superior performance seen when whole RF contours were compared to their component parts.

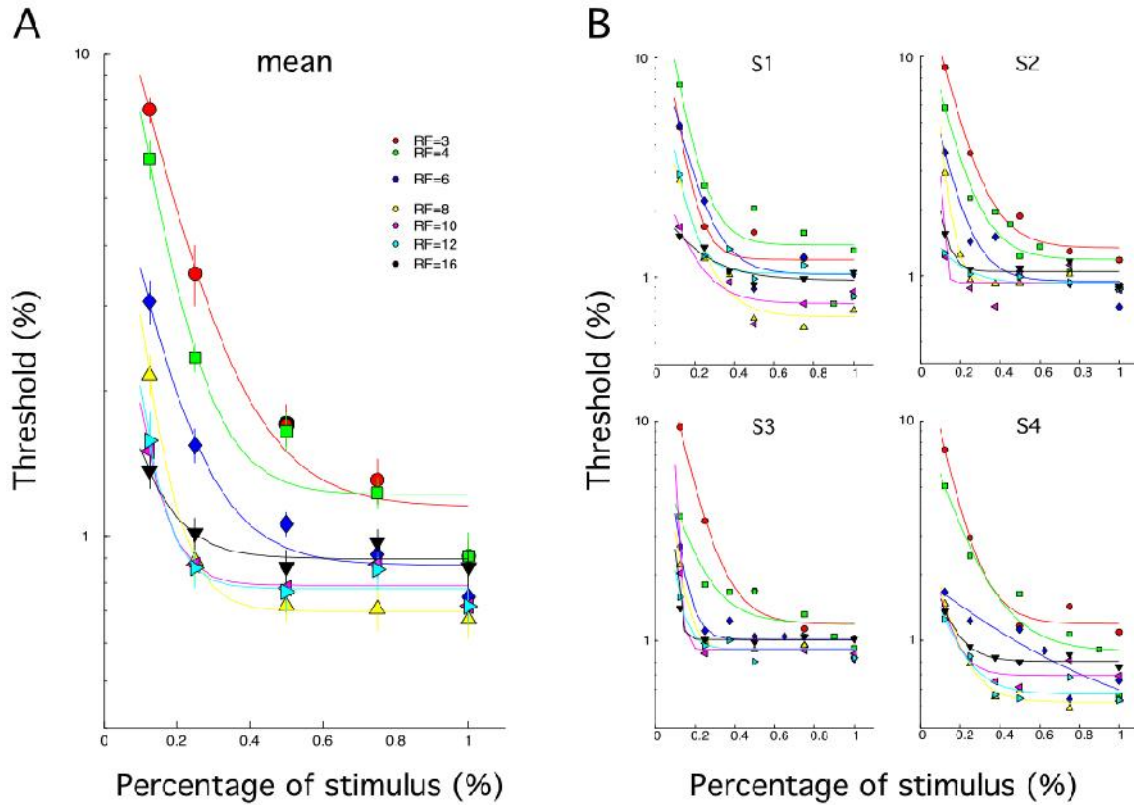


Figure 5 (a-d): % radial amplitude modulation plotted as a function of component RF fractions with contrast set at 5 X detection threshold. Threshold was significantly increased for RF patterns with local components (0.125 and 0.25).

## CHAPTER FOUR

### DISCUSSION

Results from this study are consistent with an efficient global integration mechanism summing local responses along the circumference of an RF contour. Similar conclusions have been made by several authors. Threshold for most RF patterns were clearly in the hyper-acuity range which suggests that humans are exquisitely sensitive to minute deviations from circularity and this has been roundly demonstrated by various studies (Wilkinson et al., 1998; Loffler, 2008; Bell and Kingdom, 2009; Bell et al., 2007; 2009; 2010; Schmidtman et al., 2012).

In this study we have used RF patterns a little different from other studies; we have used various component fractions of RF3-16, and results show that threshold decreased significantly with increase in the component parts and increasing RF contours. Two-Factor ANOVA showed significant differences in threshold with RF component parts and RF cycles. For all combinations of RF3 to RF16, Tukey's post-hoc test showed that there was a significant difference in threshold. Data showed that there was more variability in threshold for RF3 to RF8; although threshold for higher RF patterns looked marginal, it was nonetheless significant. On the other hand, in factor 2 (component fractions), there was no significant difference between component 0.125 and 0.25 ( $p > 0.05$ ), all other combinations were however significant ( $p < 0.01$ ). Similarly, Schmidtman et al., (2012), using repeated measures ANOVA found that threshold decreased significantly as the number of cycles of RF3 and RF5 patterns increased. Dickinson et al., (2012) also demonstrated that threshold for RF3 patterns were significantly different for one cycle open ( $q = 6.92$ ,  $p < 0.05$ ) and closed ( $q = 5.54$ ,  $p < 0.05$ ) with ANOVA after transforming their data. The significant differences seen in threshold with various component



parts in comparison to the whole, and also seen in RF3 to 16 cannot be accounted for by consideration of integration of signals from only local detectors but indicates a more global mechanism summing responses from the circumference of the patterns.

The strong negative correlation between component fractions and threshold for various RF patterns is further indication of the decrease in threshold as the fractions of the component parts increase. It is important to note that this correlation weakened marginally as higher RF cycle patterns were used ostensibly because data became more non-linear as more global aspects of the RF patterns were revealed. Schidtmann et al., (2012) also found such non-linearity in their data and concluded that it could be accounted for by a more efficient global process enabling an increased performance of the whole RF pattern in comparison to its local components.

Dickinson et al., (2012) in providing further evidence that local cues to shape in RF patterns are integrated globally used threshold ratios between single cycle open RF patterns and completely modulated RF3 pattern and found on the average a ratio of 2.8. If there was a lack of a more efficient global mechanism one will expect that the ratio between local aspects of the contour to that of the whole will be close to unity. Using our different fractions of open RF patterns, we demonstrated for RF3 pattern an average ratio of 5.96 for the 0.125 to the whole RF pattern, a result that is consistent with an efficient global integration mechanism.

Local noise within detectors could result in improved performance (decrease in threshold) and this could be misconstrued as evidence of a global mechanism, therefore many studies have used the reciprocal of the slope of the psychometric function as a measure of the strength of

integration. This slope must exceed that predicted by probability summation for an efficient global mechanism to be assumed. Probability summation prediction could be derived by taking the average slope of the psychometric function, and this slope was calculated to be about -0.33 by Graham and Robson, 1987. Other studies have used probability prediction different from -0.33. For example, Dickinson et al., (2012) used -0.44. We calculated a predicted probability summation of -0.48 for this study and as demonstrated in the result, the derived slope for the RF3 to 8 contours were significantly steeper than what would be expected by local integration predicted by probability summation.

Decreasing contrast to 5 X detection threshold did not compromise global integration as seen in experiment 2. There was however a decline in performance when smaller component fractions (0.125 and 0.25) were tested; this was even more marked with RF3 patterns. Despite the increase in threshold for smaller components, two-way ANOVA showed a statistically significant decrease in threshold with RF patterns and component fractions. The ratio of the decline in threshold from local component to that of the whole was significantly steep enough to suggest an efficient integration mechanism as would be expected from an intermediate shape processing mechanism summing inputs globally. The findings of Dickinson et al., (2012) and Schmidtman et al., (2011) support our conclusion. Both aforementioned studies also suggested that the differences seen in the results and subsequent conclusions of Mullen, Beaudot and Ivanov, (2011) could be accounted for by the fact that their methodology was different than those used in other studies since they used smooth Gaussian windowed sectors viewed in cosine phase (rather than in sine phase) to render parts of their stimuli invisible. We have also shown that threshold is affected when progressively larger component parts are

removed from the RF contour and that doing so increases threshold or reduces the ability to discriminate modulated sectors from unmodulated ones.

### **Conclusion**

This study further confirms the existence of a global shape processing mechanism summing information around the RF pattern and consequently demonstrates a greater saliency of whole RF patterns in comparison to its component parts.

## PART TWO

### CHAPTER FIVE

#### EFFECT OF SUDDEN ONSET GLARE ON SHAPE DISCRIMINATION

##### INTRODUCTION

In normal eyes, Intraocular light scatter from light emanating from a glare source results in a veiling glare over the retina that degrades retinal image quality by contrast reduction of the retinal image; this ultimately reduces visual performance and is classified as disability glare (Aslam et al., 2007; Anderson and Holladay, 1995; Gary and Regan, 2007; Wood et al., 2012; Yuan et al., 1993; Mainster and Turner, 2012; van den Berg, 1991; van den Berg et al., 2013; Franssen et al., 2007;). This reduction of visual performance is even more significant in diseases that compromise the integrity of the ocular media, the most common example being cataract (van der Meulen et al., 2012; Paulsson and Sjostrand, 1980). Apart from cataract, other conditions that have been reported to lead to an increase in intraocular light scattering are Peripheral Iridectomy (Congdon et al., 2012), LASIK (Niesen et al., 1996), IOL in pseudophakia (Peng et al., 2012) just to mention a few.

The equivalent veiling luminance has been used to quantify the veiling glare over the retina (Holladay, 1927; Vos et al., 2002) in the intraocular milieu and is given by the equation below:

$$L_{eq} = 9.2 \sum_{i=1}^n E_i / \Theta_i (\Theta + 1.5) \text{-----} (3)$$

$L_{eq}$  is the equivalent luminance;  $E_i$  is the illuminance from the  $i$ th glare source in Lux, while  $\Theta$  is the angle between the fixation point and the glare source (Figure 6). If we assume a perfect

modulation transfer function for the normal eye then the contrast of the retinal image will equal that of the contrast of the target stimulus. Thus contrast will be:

$$C = (L_{\max} - L_{\min}) / (L_{\max} + L_{\min}) \text{-----(4)}$$

C is the retinal image contrast,  $L_{\max}$  is the maximum luminance and  $L_{\min}$  is the minimum luminance.

To quantify the effect veiling glare will have on retinal image contrast which is a reduction as already mentioned, the equivalent luminance will have to be added to contrast as in equation 5:

$$\begin{aligned} & [(L_{\max} + L_{eq}) - (L_{\min} + L_{eq})] / [(L_{\max} + L_{eq}) + (L_{\min} + L_{eq})] \\ & = (L_{\max} - L_{\min}) / (L_{\max} + 2L_{eq}) \text{-----(5)} \end{aligned}$$

where  $L_{eq}$  represents the equivalent luminance. Another mathematical model for equivalence luminance was provided by Paulsson and Strostrand 1980:

$$\eta = (L/E)(M_2/M_1 - 1) \text{-----(6)}$$

$\eta$  is the scattering factor (equivalent luminance) and is a function of  $\Theta$  in equation 1; L is the mean luminance of the target stimulus; E is the luminance of the glare source;  $M_1$  and  $M_2$  are the contrast with and without glare respectively of the retinal image if one assumes ideal modulation transfer function.

It is obvious from equation 5 that the equivalent luminance from intraocular light scattering when added to retinal image contrast will degrade retinal image quality (contrast) and decrease visual performance as a consequence.

Most studies have used visual acuity as a measure of visual performance when studying the effect of glare while some have used the contrast sensitivity function (Gary and Regan, 2007). This appears to be the first time radial frequency patterns have been used to study the effect of sudden onset glare on shape discrimination as far as we can determine. Two major experiments were performed. The first part of experiment 1 studied the effect of sudden onset glare on the threshold of closed RF3 and RF4 contours in a shape discrimination task. The second part of experiment 1 used equivalent low contrast RF3 and RF4 contours to study whether the veiling luminance model can account for the effect of glare on threshold in a shape discrimination task. The third part of experiment 1 studied the effect of changes in the mean luminance level on the aforementioned parts. Experiment 2 studied the effect of glare on the threshold of discriminating open fractions of the RF contours in a shape discrimination task and at both high and low mean luminance levels. This study provides evidence that sudden onset glare increases the threshold of shape discrimination and that the equivalent luminance model does not fully account for the decrease in visual performance using radial frequency stimuli.

## CHAPTER SIX

### Method

#### Apparatus

All stimuli were generated using Matlab 2010b (Mathworks) and Psychtoolbox (Bernard, 1997; Peli, 1997). The host computer is Windows 7 based PC (Dell Optiplex, 780). All stimuli are displayed on a gamma corrected CRT monitor (Richard Electronics, 15.3" W X 11.5" H), with resolution of 1280 X 1024 and a refresh rate at 100 Hz. The luminance of the pattern was 50 cd/m<sup>2</sup> while contrast was linearized at 256 equally spaced grey levels. Subjects were seated 60 cm from the computer monitor in ambient illuminance condition with chin placed in the chin rest and forehead on the forehead rest to maintain a stable fixation distance. At this distance the stimuli covered an area of about 512 X 512 pixels.

#### Stimuli

The stimuli were radial amplitude modulation of the radius of a circle derived using equation (1)

$$R(\Theta) = r_0[1 + A\sin(\omega\Theta + \Phi)] \text{-----(1)}$$

A is the radial modulation amplitude,  $\omega$  is the radial frequency,  $\Phi$  is the angular phase, while  $\Theta$  represents the polar coordinates. The radial modulation amplitude (A), determines how distinct the pattern is; the radial frequency ( $\omega$ ), determines the number of lobes the pattern has; and the phase angle ( $\Phi$ ), determines the orientation of the pattern (Figure 1). The equation generates a perfect (unmodulated) circle when amplitude is set at zero. The amplitude A was always set between 0 and 1 to prevent the crossing of the closed patterns; also the phase of the pattern was varied to ensure subjects were not able to predict the position of the lobes.

The cross-sectional luminance profile of the RF pattern used in this study is defined by the fourth derivative of Gaussians (D4) and represented by the equation 2 below:

$$D4(r) = C\{1 - 4[(r - r_0)/\sigma]^2 + (4/3)(r - r_0)/\sigma\}^4 \exp[-((r - r_0)/\sigma)^2] \text{-----}(2)$$

C is the contrast of the contour, r and r<sub>0</sub> is the radius and mean radius respectively, while σ determines the peak spatial frequency which was set at 8cpd for this study, full spatial frequency bandwidth at half amplitude was 1.24 octaves. The partial RF contours used in experiment 2 were generated by restricting RF3 contours between specific polar angles (Θ, in equation 5).

The amount of light was set at mesopic levels. The glare source was the Integrated Glare Testing System (M&S Technologies, IL). The propriety lenses minimize the light “spray”, starburst and halo effects created by the glare system. The center of the glare source was the same height as the stimulus and deviated horizontally by 10° from the visual axis. The observers wore artificial pupils of 1.5 mm in diameter to ensure uniform retinal luminance. The amount of glare entering the eye was calculated using the Stile-Holladay formula:

$$L_{eq}(\Theta) = (10 * E / \Theta^2) \text{ for } 1^\circ < \Theta < 30^\circ \text{-----}(7)$$

Where L<sub>eq</sub> is the equivalent veiling luminance; E is the illumination of the glare source (Lux) incident of the cornea, and Θ is the angle between the visual axis and the glare source (degrees).



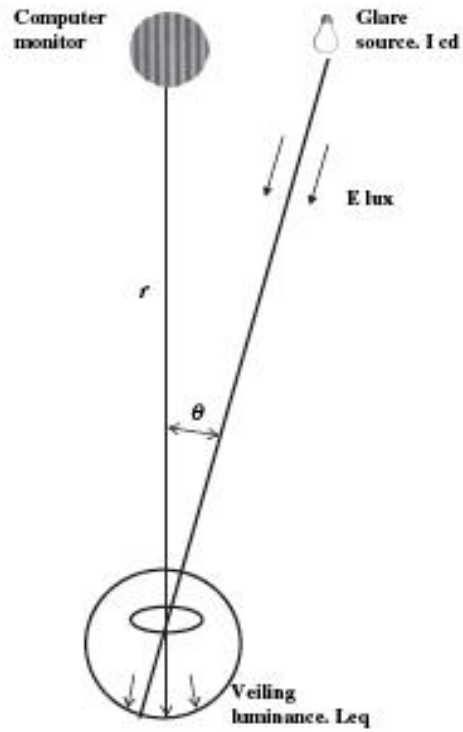


Figure 6. Schematic representation of the experiments. Glare source is separated from the test monitor by the angle  $\Theta$ . Intraocular light scattering (retinal straylight) causes a veiling glare over retinal image, degrading its quality.

## Experimental Protocol

The procedure used in this study was the temporal two-alternative forced choice (2AFC) paradigm. The reference and test contours were randomly presented to ensure the subjects could not predict the test pattern based on which one comes first. The time lapse between the presentation of the reference pattern and test pattern was 160ms and the inter-stimulus presentation time was 300ms. The task of the subjects was to discriminate between modulated ( $A > 0$ ;  $A < 1$ ) and unmodulated ( $A = 0$ ) patterns. Six modulation amplitudes including, 0.20, 0.3, 0.4, 0.5, 0.75 and 1.0 were used, with each amplitude tested 30 times, making a total of 180 presentations per experiment. The response criterion was that the amplitude was decreased after two correct responses and increased after one wrong response. The responses of the subjects were automatically recorded when they pressed the left pointing arrow key on the computer key-board indicating that the first presentation was the modulated pattern or when they pressed the right pointing arrow key indicating that the second presentation was the modulated pattern. No feedback was given to the subjects. For each amplitude modulation point, threshold was computed for 62.5% correct response using the maximum likelihood psychometric analysis and fitted with the Weibull model. Bootstrap analysis of 500 simulations indicated that the model was good fit. All procedures were carried out without and with the glare source on.

## Experiment 1

Five subjects made up of 4 experienced psychophysical test takers and 1 naïve observer took part in the study. The stimuli were RF3 and RF4 contours and the task of subjects was to discriminate modulated pattern from an unmodulated circle, with or without glare present (Figure 7). The RF contours were either high contrast stimuli set at 20% (20 times detection threshold), or the equivalent low contrast stimuli set at 5% (5 X detection threshold).

The purpose of this experiment was to study the effect of sudden onset glare on the threshold of discriminating closed RF contours, while the rationale for using the equivalent low contrast contour (set at 5 X detection threshold) was to determine if the veiling glare or retinal straylight model alone accounts for changes in threshold position. Having calibrated the exact luminance from the glare source that will result in a veiling glare expected to reduce the contrast of the high contrast contour to that of the equivalent low contrast pattern, we should then expect that shape discrimination threshold for the high contrast (20%) stimulus with the glare source on will not be significantly different from threshold for the low contrast (5%) stimulus without glare. Stated differently, our null hypothesis was that there is no significant difference between shape discrimination with glare for the high contrast stimulus RF pattern and that of low contrast stimulus without glare. To test the effect changes in mean luminance levels will have on shape discrimination threshold, the high contrast stimuli were set at 10% (10 X detection threshold) closer to the equivalent low contrast stimuli.

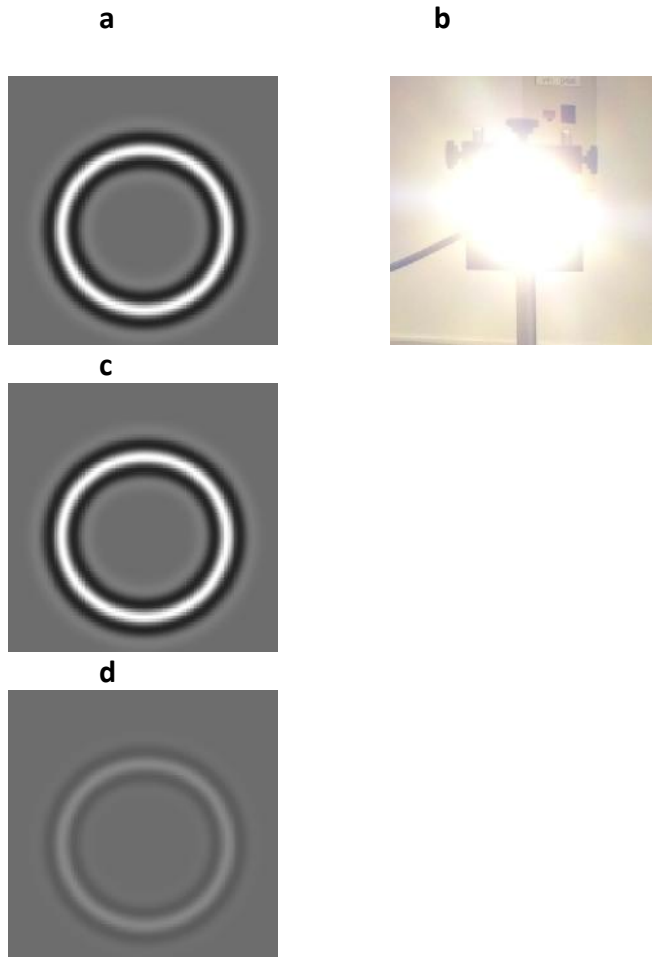


Figure 7. a. unmodulated high contrast RF contour with glare; b. glare source; c. unmodulated high contrast contour without glare; d. equivalent low contrast RF contour. The glare source renders the contrast of a to be equal to that of d.

## Experiment 2

In experiment 2 different fractions of RF3 and RF4 contours corresponding to 0.50 and 0.75 of the whole and set at 5% contrast were used as stimuli. The task for the subjects was to discriminate between modulated fractions against unmodulated reference patterns.

**Subjects**

All subjects had normal or corrected to normal acuities and had neither ocular pathologies nor binocular vision anomalies. They all underwent 2 practice sections before the actual experiments.

**Declaration**

The study was approved by the Nova Southeastern University Institutional review board (IRB) and done in accordance with the Helsinki declaration of the use of human subjects.

## CHAPTER SEVEN

### RESULTS

The red dots represent threshold with high contrast stimuli (20 X detection threshold) in the presence of glare; the grey dots represent threshold for the equivalent low contrast stimulus (5 X detection threshold) without glare; the black dots represent threshold for the high contrast (20 X detection threshold) without glare. Figure 8 is a display of results of threshold points from experiment 1. All threshold points for high contrast RF contours without glare (black dots) were quite low, at hyper-acuity ranges. RF3 contours however had slightly elevated threshold points compared to RF4 at high mean luminance levels (Figs. 8A and 8B). The highest threshold points demonstrated were those of high contrast contours in the presence of glare (red dots). This indicates that sudden glare significantly degraded the performance of this shape discrimination task. Interestingly, threshold of high contrast contours in the presence of glare was higher than that of the equivalent low contrast low contrast contour. The equivalent low contrast contour was carefully constructed to ensure that it has the same contrast as that of the high contrast contour when glare impinges on the retina. In effect, it means that equal performance should be expected with the high contrast contour with glare and the equivalent low contrast contours if the veiling luminance alone is responsible for the reduced visual performance (higher threshold). The results show to the contrary that performance with the equivalent low contrast contour was better (lower threshold) than that of the high contrast contour in the presence of glare. This clearly demonstrates that the veiling luminance model alone cannot fully account for the reduction in visual performance.

Thus far the study has demonstrated a consistent increase in threshold or a reduction in visual performance in the presence of glare at high mean luminance level (20 X detection threshold), the second part of experiment 1 used contours with a lower mean luminance (10 X detection threshold), and again a significant increase in threshold for shape discrimination was demonstrated (Fig. 8C, D). What this represents is that irrespective of the luminance parameters of an object in space, glare is expected to increase the threshold of accurately discriminating its shape. Figures 8C and D also show that the threshold increase is more significant with the RF3 contour when compared to that of RF4.

A two-way analysis of variance (ANOVA) was performed first for the 20% contrast data. The first factor was called the contrast factor with three levels, high contrast plus glare, high contrast without glare and equivalent low contrast. The second factor was the RF contour used and has two levels, RF3 and RF4. Threshold was significantly different between RF patterns ( $p < 0.01$ ); RF4 thresholds were significantly lower than RF3 thresholds indicating that the subjects were better at discriminating RF4 modulated patterns from perfect circles than they were in discriminating RF3 patterns. There was a significant difference in threshold across contrast levels ( $p < 0.01$ ). ANOVA post-hoc with Tukey's test showed threshold for high contrast target with glare was significantly higher than that of equivalent low contrast target ( $p = 0.014$ ). There was also a significant difference in threshold between high contrast target with glare and high contrast target without glare ( $p < 0.01$ ). Furthermore there was a significant difference in threshold between high contrast target without glare and equivalent low contrast target ( $p = 0.012$ ). There was no significant interaction between the two factors ( $p > 0.05$ ).

A separate 2-way ANOVA was performed for data with contrast set at 10%. Threshold for RF4 contours were significantly lower than that of RF3 contours ( $p < 0.01$ ); threshold also varied significantly with contrast levels ( $p < 0.01$ ) and there was no significant interaction between the two factors ( $p = 0.26$ ). Tukey's post-hoc test revealed a significant difference between high contrast target with glare and equivalent low contrast target ( $p = 0.033$ ) and between high contrast targets with or without glare ( $p < 0.01$ ). Post-hoc comparison of threshold between high contrast targets without glare was also significantly lower than that of the equivalent low contrast target ( $p = 0.019$ ).

Results for experiment 2 are plotted in Figures 9A-D. The figures show that when fractions, 50% (a) and 75% (b), of the low contrast RF4 contours were tested, threshold increased. The increase was higher the larger the missing sector, with the threshold for the 75% approximating that of the high contrast target in the presence of glare. The same trend was seen with RF3 contours but threshold with the RF3 contours were significantly higher by comparison. Figure 9C and D show results when fractions of low contrast RF3 and RF4 contours were tested at different mean luminance levels. Again, similar trend as reported earlier were demonstrated: threshold increased the larger the missing sector; RF3 threshold were higher and low mean luminance level generally ramped up threshold.

Putting all the results together, this study has demonstrated that glare reduced visual performance in the task of shape discrimination. That this reduction is even more significant when partial contours are tested and even more so at low mean luminance levels. We have also demonstrated that since threshold with high contrast contours in the presence of glare is significantly higher than that of equivalent low contrast contours we can reject our null



hypothesis and conclude that our data could not account for the veiling luminance as the only source of the reduction in visual performance in this shape discrimination task.

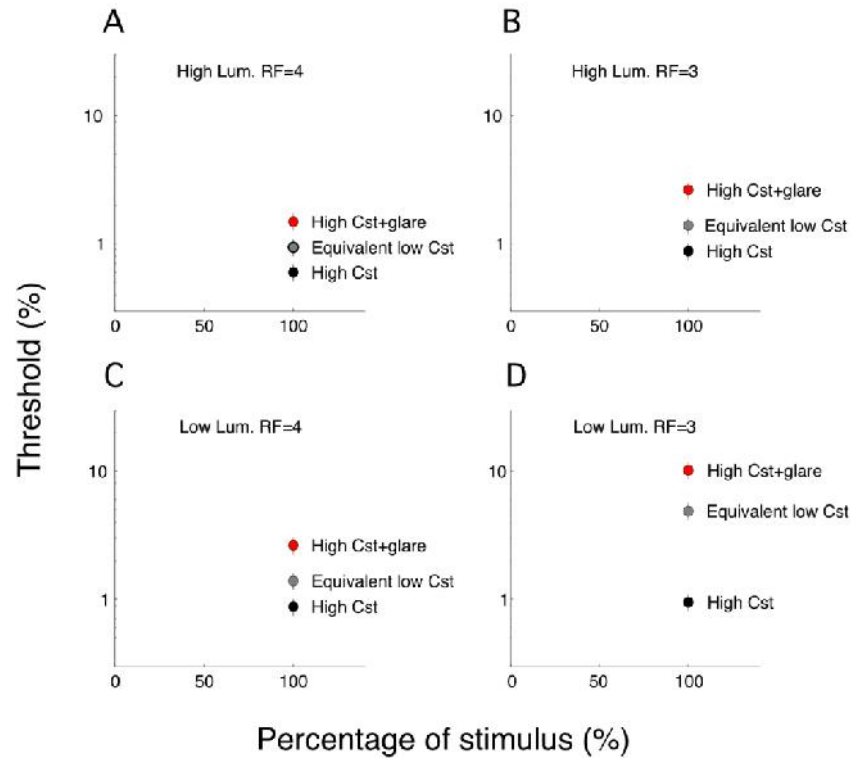


Figure 8. Threshold points for high contrast RF and equivalent low contrast contours. High contrast contour in the presence of glare (red dot); high contrast contour in the absence of glare (Black dot); equivalent low contrast contour (grey dot). A and B were tested at high mean luminance level, while C and D were tested at low mean luminance level.

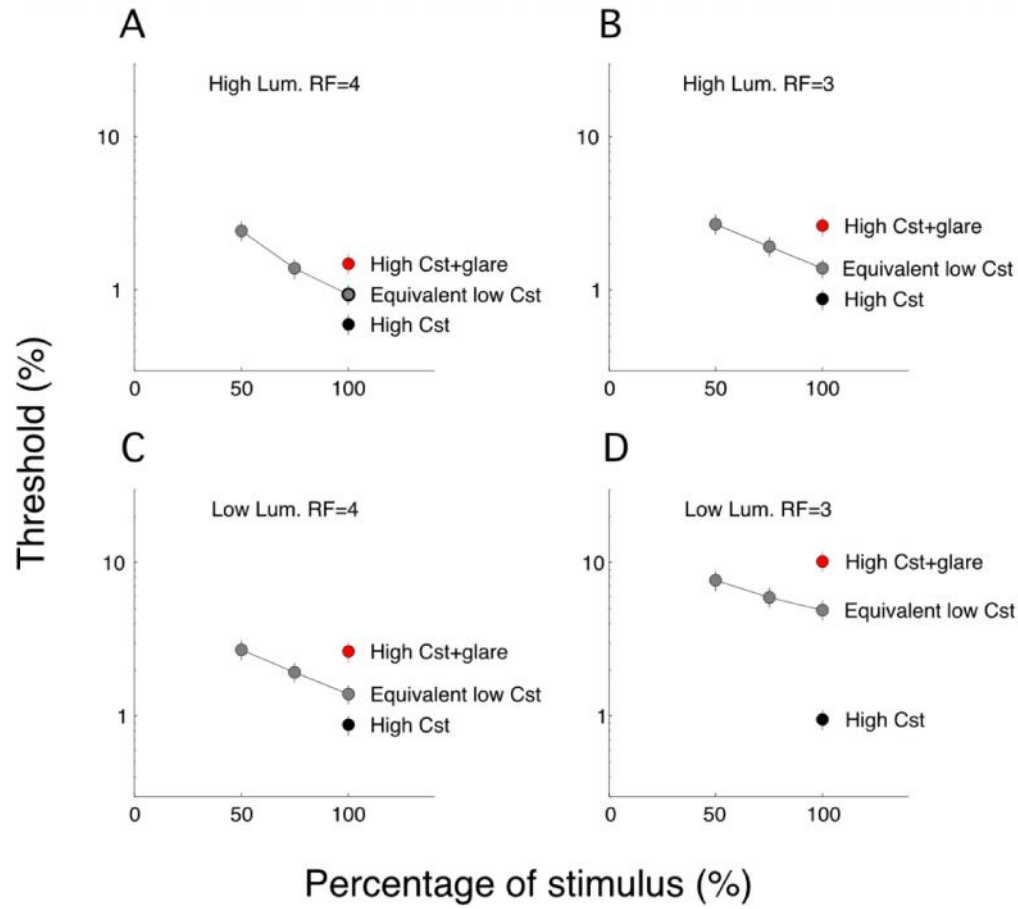


Figure 9. All plots show equivalent luminance contour tested using partial open contours (50 and 75%). Plots A and B are at high mean luminance levels while C and D were tested at low mean luminance levels.

## CHAPTER EIGHT

### DISCUSSION

The literature is replete with evidence supporting a reduction in various aspects of visual performance as a result of glare. The reduction has been attributed to veiling luminance or retinal straylight reducing the contrast and thus the quality of the retinal image (Anderson and Holladay, 1995; Aslan et al., 2007; Congdon et al., 2012; Mainster, 2012; van den Berg, 2013; van den Meulen, 2012). Paulsson and Strostrand (1980) demonstrated a reduction in contrast sensitivity function in the presence of glare, a reduction that was even more significant in patients with cataract. Anderson and Holladay, (1995) in their study on the effect of glare from vehicle headlights showed a significant decrease in motion perception. Aguirre et al., (2008) in evaluating the influence of glare on suprathreshold visual performance using simple reaction times in a detection task noted an increase in simple reaction times which indicates a decrease in visual performance.

This study appears to be the first time, as far as we know, that used RF patterns to study the effect of glare on visual performance in a shape discrimination task. We have demonstrated that sudden onset glare does indeed increase the threshold of discriminating the RF shapes, and this difficulty increases when local components of the contour are tested, as seen by the fact that threshold of smaller open contours are higher than those of whole closed ones. Lower mean luminance also increases threshold of discriminating RF contours across the board irrespective of RF type or whether they are open fractions or closed whole contours.

Some studies have looked at the role of the veiling luminance model as the sole cause of the increase in threshold in visual performance tasks and have found that veiling luminance alone

does not fully account for the reduction in visual performance. Aguirre et al., (2008) found that sudden glare increases simple reaction times (RT) in a detection task but when the data was plotted as a function of the inverse of contrast there was a linear relationship between RT and the slope of the graph. Glare increased the slope of the graph but interestingly, the slope varied with spatial frequency which is not what one would expect if the veiling luminance over the retinal image is the only source of vision compromise. Paulsson and Strostrand, (1980) used the contrast sensitivity function (CSF) of normal subjects and those with varying degrees of cataract and used the veiling luminance model imposed by the glare source to account for the reduction in visual perception, a reduction that was even more marked in individuals with cataract. It is however striking to note that their result showed a disparate reduction in CSF in the spatial frequency domain with many of the subjects showing more distinct reduction in the low and medium frequency ranges. If the veiling luminance alone explains the reduction of visual performance such spatial frequency selectivity will not be seen but instead a uniform reduction in CSF would have been demonstrated.

Our data showed that the veiling luminance model could not completely account for the reduction in the shape discrimination threshold. In experiment 1 we demonstrated that shape discrimination threshold for high contrast targets in the presence of a glare source was significantly higher than that of equivalent luminance target, which is contrary to what is expected since the veiling luminance imposed by the glare source reduces the contrast of the high contrast target to that of the equivalent luminance target. This same result was replicated even when a target with a contrast of 10 X the detection threshold was used. What this implies is that the effect of glare on a target is not dependent on the contrast of the target and that

performance in the presence of a glare source is worse than without glare at an equivalent contrast level. Furthermore there was no significant difference in threshold when open contour (1/2 or 3/4) targets at low contrast levels (in the absence of glare) were compared to that of closed high contrast targets (in the presence of glare).

## **Conclusion**

This study showed that transient glare significantly impaired ability to detect minute radial deformation of an RF contour, furthermore that the impairment was significantly greater than that caused by contrast reduction and finally that the impairment caused by transient glare was similar to those measured at low contrast with sections of the contours missing. Data modeled by using the veiling luminance over the retinal image, alone could not account for the reduction of visual performance.

## BIBLIOGRAPHY

- Adamson P. Arabic Sciences and philosophies- Vision, light and color in al-Kindi, Ptolemy and the ancient commentators. New York, 2006.
- Aguirre RC, Colombo EM and Barraza JF. Effect of glare on simple reaction time. *J Opt Soc Am. A/Vol 25*, 7 Jul 2008.
- Albus K and Fries W. Inhibitory sidebands of complex receptive fields in the cat's striate cortex. *Vision Res.* 20: 369-372, 1980.
- Anderson SJ, Holladay IE. Night driving: effects of glare from vehicle headlights on motion perception. *Ophthalmic Physiol Opt.* 15(6): 545-51, Nov 1995.
- Aslan TM, Haider D, Murray IJ. Principles of disability glare measurement: an Ophthalmological perspective. *Acta Ophthalmol Scand.* 85(4): 354-60, Jun 2007.
- Bell J and Kingdom FAA. Global contour shapes are coded differently from their local components. *Vision Research* 49 1702–1710, 2009.
- Bell J, Badcock DR, Wilson H and Wilkinson F. Detection of shape in radial frequency contours: independence of local and global form information. *Vision Research* 47 1518–1522. 2007.
- Bell J, Hancock S Kingdom FAA and Peirce JW. Global shape processing: Which parts form the whole? *Journal of Vision* 10(6):16, 1–13, 2010.
- Bell J, Wilkinson F, Wilson HR, Loffler G and Badcock DR. Radial frequency adaptation reveals interacting contour shape channels. *Vision Research* 49 2306–2317, 2009.
- Bernard DH. The Psychophysical Toolbox, *Spatial Vision* 10: 433-436, 1997.
- Blakemore CB, and Tobin EA. Lateral inhibition between orientation detectors in the cat's visual cortex. *Exp. Brain Res.* 15: 439-440, 1972.
- Bolz J and Gilbert CD. Generation of end-inhibition in the visual cortex via interlaminar connections. *Nature Land.* 320: 362-365, 1986.
- Bonds, A. B. (1989). Role of inhibition in the specification of orientation selectivity in the cat striate cortex. *Visual Neuroscience*, 2, 41–55.
- Bonds, A. B. (1991). Temporal dynamics of contrast gain in single cells of the cat striate cortex. *Visual Neuroscience*, 6, 239–255.
- Born RT and Tootell RBH. Single-unit and 2-deoxyglucose studies of side inhibition in macaque striate cortex. *Proc. Natl. Acad. Sci. USA* 88:7071-7075, 1991.

Brincat SL and Connor CE. Underlying principles of visual shape selectivity in posterior inferotemporal cortex. *Nature Neuroscience*, 7(8), 880–886, 2004.

Congdon N, Yan X, Friedman DS, Foster PJ, van den Berg TJ, Peng M, Gangwani R, He M. Visual symptoms and retinal straylight after laser peripheral iridotomy: the Zhongshan Angle-Closure Prevention Trial. *Ophthalmology*. 119(7):1375-82, Jul 2012.

Das A and Gilbert CD. Long-range horizontal connections and their role in cortical reorganization revealed by optical recording of cat primary visual cortex. *Nature*, 375(6534), 780–784, 1995.

Das A and Gilbert CD. Topography of contextual modulations mediated by short-range interactions in primary visual cortex. *Nature*, 399, 655–661, 1999.

Desimone R. Face-selective cells in the temporal cortex of monkeys. *Journal of Cognitive Neuroscience*, 3(1), 1–8, 1991

De Valois R, Albrecht D, and Thorell L. Spatial frequency selectivity of cells in macaque visual cortex. *Vision Research*, 22, 545–559, 1982

Devalois RL, Thorell LG, and Albrecht DG. Periodicity of striate cortex cell receptive fields. *J. Opt. Soc. Am. 2*: 1 115- 1122, 1985.

Dickinson EJ, McGinty J, Webster KE and Badcock DR. Further evidence that local cues to shape in RF patterns are integrated globally. *Journal of Vision* 12(12): 16, 1-17, 2012

Dreher B. Hypercomplex cells in the cats striate cortex. *Invest Ophthalmol Visual Sci* 11: 355-356, 1972.

Dumoulin SO, and Hess RF. Cortical specialization for concentric shape processing. *Vision Research*, 47(12), 1608–1613, 2007.

Elder JH, and Goldberg RM. Ecological statistics of Gestalt laws for the perceptual organization of contours. *Journal of Vision*, 2(4), 324–353, 2002.

Gallant JL, Braun J, and Vanessen DC. Selectivity for polar, hyperbolic, and Cartesian gratings in macaque visual-cortex. *Science*, 259(5091), 100–103, 1993.

Franssen L, Taberner J, Coppens JE, van den Berg TJ. Pupil size and retinal straylight in the normal eye. *Invest Ophthalmol Vis Sci*. 48(5):2375-82, May 2007.

Fries W, Albus K, and Creutzfeldt OD. Effects of interacting visual patterns on single cell responses in cat's striate cortex. *Vision Res*. 17: 1001-1008, 1977.



Gallant JL, Braun J and Vanessen DC. Selectivity for polar, hyperbolic, and Cartesian gratings in macaque visual-cortex. *Science*, 259(5091), 100–103, 1993.

Gallant JL, Shoup RE, and Mazer JA. A human extrastriate area functionally homologous to macaque V4. *Neuron*, 27(2), 227–235, 2000.

Gary R and Regan D. Glare susceptibility test results correlate with temporal safety margin when executing turns across approaching vehicles in simulated low-sun conditions. *Ophthalmic Physiol Opt.* 27(5): 440-50 Sep 2007.

Geisler WS, Perry JS, Super BJ, and Gallogly DP. Edge co-occurrence in natural images predicts contour grouping performance. *Vision Research*, 41(6), 711–724, 2001.

Gilbert CD. Laminar differences in receptive field properties of cells in cat primary visual cortex. *J. Physiol. Land.* 268: 39 I-42 1, 1977.

Goodale MA, and Milner AD. Separate visual pathways for perception and action. *Trends in Neurosciences*, 15(1), 20–25, 1992.

Gross CG. Representation of visual-stimuli in inferior temporal cortex. *Philosophical transactions of the Royal Society of London Series B-Biological Sciences*, 335(1273), 3–10, 1992

Grusser OJ. Interaction of efferent and afferent signals in visual perception: A history of ideas and experimental paradigms. *Acta Psychologica.* 63(1); 3-21, Dec 1986.

Habak C, Wilkinson F, Zakher B, and Wilson HR. Curvature population coding for complex shapes in human vision. *Vision Research*, 44(24), 2815–2823, 2004.

Hatch RA. The scientific revolution: Theories of vision. <http://web.clas.ufl.edu/users/ufhatch/pages/03-Sci-Rev/SCI-REV-Home/resource-ref-read/vision/08sr-vision.htm>

Heeger D. J. Normalization of cell responses in cat striate cortex. *Visual Neuroscience*, 9, 181–197, 1992.

Hubel D and Wiesel T. Receptive fields, binocular interaction, and functional architecture in the cat's visual cortex. *Journal of Physiology (London)* 160, 106-154, 1962.

Hubel DH and Wiesel TN. Receptive fields and functional architecture in two nonstriate visual areas (18 and 19) of the cat. *Journal of Neurophysiology*, 28, 229-289, 1965.

Hubel DH and Wiesel TN. Receptive fields and functional architecture of monkey striate cortex. *Journal of Physiology*, 195, 215-243, 1968.

Kato H, Bishop P O, and Orban GA. Hypercomplex and simple/complex cell classifications in cat striate cortex. *J. Neurophysiol.* 41: 1071-1095, 1978.

Kayaert G, Biederman I, and Vogels R. Shape tuning in macaque inferior temporal cortex. *Journal of Neuroscience*, 23(7), 3016–3027, 2003.

Loffler G. Perception of contours and shapes: Low and intermediate stage mechanisms. *Vision Research* 48 2106–2127, 2008.

Loffler G, Wilson HR, Wilkinson F. Local and global contributions to shape discrimination. *Vision Research* 43 519-530, 2003.

Loffler G, Yourganov G, Wilkinson F, and Wilson HR. fMRI evidence for the neural representation of faces. *Nature Neuroscience*, 8(10), 1386–1390, 2005.

Maffei L and Fiorentini A. The unresponsive regions of visual cortical receptive fields. *Vision Res.* 16: 1131-1139, 1976.

Mainster MA, Turner PI. Glare's causes, consequences and clinical challenges after a century of Ophthalmic study. *Am J Ophthalmol.* 153(4) 587-93, Apr 2012

Mullen KT, Beaudot WHA and Ivanov IV. Evidence that global processing does not limit thresholds for RF shape discrimination. *Journal of Vision* 11(3):6, 1–21, 2011.

Mullen KT and Beaudot WHA. Comparison of color and luminance vision on a global shape discrimination task. *Vision Research* 42 565–575, 2002.

Nelson, JI and Frost BJ. Orientation-selective inhibition from beyond the classic visual receptive field. *Brain Res.* 139: 359-365, 1978.

Niesen UM, Businger U, Schipper I. Disability glare after excimer laser photorefractive keratectomy for myopia. *J Refract Surg.* 12(2):S267-8, Feb 1996.

Orban GA, Kato H, and Bishop PO. End-zone region in receptive fields of hypercomplex and other striate neurons in the cat. *J. Neurophysiol.* 42: 8 18-832, 1979a.

Orban GA, Kato H, and Bishop, PO. Dimensions and properties of end-zone inhibitory areas in receptive fields of hypercomplex cells in cat striate cortex. *J. Neurophysiol.* 42: 833-849, 1979b.  
Pastore N. Selective history of theories of visual perception, 1650-1950. London, 1971.

Pasupathy A, and Connor CE. Shape representation in area V4: Position specific tuning for boundary conformation. *Journal of Neurophysiology*, 86(5), 2505–2519, 2001.

Paulsson and Sjostrand. Contrast Sensitivity in the presence of a glare light: theoretical concepts and preliminary clinical studies. *Invest Ophthalmol Vis Sic* 19(4) 401-406, Apr 1980.

Pelly DG. The Video Toolbox software for visual psychophysics: Transforming numbers into movies. *Spatial Vision* 10: 437-442, 1997.

Polat U and Sagi D. The architecture of perceptual spatial interactions. *Vision Research*, 34(1), 73–78, 1994.

Rose D. Responses of single units in cat visual cortex to moving bars as a function of bar length. *J. Physiol. Lond.* 27 1: 1-23, 1977.

Schmidtman G, Kennedy GJ, Broach HS, Loffler G. Non-linear global pooling in the Discrimination of circular and non-circular shapes. *Vision Res.* 62:44-56, Jun 2012

Schmolesky M. The primary visual cortex. *Webvision*.  
<http://webvision.med.utah.edu/book/part-ix-psychophysics-of-vision/the-primary-visual-cortex/>

Sillito AM and Versiani V. The contribution of excitatory and inhibitory inputs to the length preference of hypercomplex cells in Layers II and III of the cat's striate cortex. *J. Physiol. Lond.* 273: 775-790, 1977.

Sillito AM. The spatial extent of excitatory and inhibitory zones in the receptive field of superficial layer hypercomplex cells. *J. Physiol. Lond.* 273: 79 1-803, 1977.

Smith MA. Knowing things inside out: The Scientific Revolution from a Medieval perspective. *American Historical review.* 95 726-744, 1990.

Tanaka K. Inferotemporal cortex and object vision. *Annual Review of Neuroscience*, 19, 109–139, 1996.

Tanaka K, Ohzawa I, Ramoa AS, and Freeman RD. Receptive field properties of cells in area 19 of the cat. *Exp. Brain Res.* 65: 549- 558, 1987.

Valentine, T. A unified account of the effects of distinctiveness, inversion, and race in face recognition. *Quarterly Journal of Experimental Psychology Section A—Human Experimental Psychology*, 43(2), 161–204, 1991.

Van den Berg TJ. On the relation between glare and straylight. *Doc Ophthalmol* 78(3-4); 177-81, 1991.

van den Berg TJ, Franssen L, Krait B, Coppens JE. History of ocular straylight measurement: A review. *Z Med Phys.* 23(1):6-20, Feb 2013.

van der Meulen IJ, Gerstein J, Krait B, Wither JP, Rule A, Schlingemann RO, van den Berg TJ. Straylight measurements as an indication for cataract surgery. *J Cataract Refract Surg.* 2012 38(5):840-8, May 2012.

Van Essen DC, Anderson CH, and Felleman DJ. (1992). Information processing in the primate visual system: An integrated systems perspective. *Science*, 255(5043), 419–423, 1992.

Von der Heydt R, Peterhans E, and Dursteler MR. Periodic pattern- selective cells in monkey visual cortex. *J. Neurosci.* 12: 14 16- 1434, 1992.

Wilkinson, F., Wilson, H. R., & Habak, C. Detection and recognition of radial frequency patterns. *Vision Research*, 38(22), 3555–3568, 1998.

Wade NJ. *A Natural history of vision.* MIT Press, Cambridge, 1999.

Wagner BT, Kline D. The bases of color vision. University of Calgary. <http://psych.ucalgary.ca/PACE/VA-Lab/Brian/history.htm>

Wilson, H. R., & Humanski, R. Spatial frequency adaptation and contrast gain control. *Vision Research*, 33(8), 1133–1149, 1993.

Wolfram S. Some historical notes from: A new kind of science. Notes for chapter 10: process of perception. <http://www.wolframscience.com/reference/notes/1076b>

Wood JM, Tyrrell RA, Chaparro A, Marszalek RP, Carberry TP and Chu SB. Even moderate visual impairments degrade driver's ability to see pedestrians at night. *Invest Ophthalmol. Vis. Sci.* 53(6): 2586-2592, May 2012.

Yamane S, Maske R, and Bishop PO. Properties of end-zone inhibition of hypercomplex cells in cat striate cortex. *EXP. Brain Res.* 60: 200-203, 1985.

Young MP. Objective analysis of the topological organization of the primate cortical visual system. *Nature*, 358(6382), 152–155, 1992.

Yu C, and Levi DM. End stopping and length tuning in psychophysical spatial filters. *Journal of the Optical Society of America A: Optics and Image Science, and Vision*, 14(9), 2346–2354, 1997a.

Yuan R, Yager D, Guethlein M, Oliver G, Kapoor N, Zhong R. Controlling unwanted sources of threshold change in disability glare studies: a prototype apparatus and procedure. *Optom vis, Sci.* 70(11): 976-81, Nov 1992

Zemlen GA. *The History of Vision, color, and light theories-Introduction, Text, problems.* Gabor A, Zemlen-Bern, 2005.

APPENDIX A

High contrast data

Subject -1

A	B	C	D	E	F	G	H	I	J	K	L
name				contrast		100%			SF=1.5 R=2.4		
proportion		2	3	4	5	6	7	8	10	12	16
0.03625											
2 cyc											
3 cyc											
4cyc											
0.0625	7.5										0.0028828
0.125	15		0.024217	0.01598		0.0071722		0.0048668	0.0031248	0.002889	0.0017313
0.15	18										
0.175	21										
0.2	24										
0.225	27										
0.25	30		0.0081025	0.0085917		0.0050548		0.0021466	0.0018887	0.0019524	0.0015455
0.275	33										
0.3	36										
0.325	39										
0.35	42										
0.375	45										
0.4	48										
0.425	51										
0.45	54										
0.475	57										
0.5	60		0.0077333	0.0046324		0.0030224		0.0020686	0.0022433	0.0018434	0.0012592
0.525	63										
0.55	66										
0.575	69										
0.6	72										
0.625	75										
0.65	78										
0.675	81										
0.7	84										
0.75	90		0.0047098	0.003		0.0032616		0.0019619	0.0021168	0.0019649	0.0015127
0.8	96										
0.875	105										
0.9	108										
0.95	114										
1	120		0.006872	0.0033757		0.0031617		0.0019868	0.0022899	0.0017906	0.0014321

APPENDIX B

Subject-2

A	B	C	D	E	F	G	H	I	J	K	L
name				contrast		100%			SF=1.5 R=2.4		
proportion		2	3	4	5	6	7	8	10	12	16
0.03625											
2 cyc											
3 cyc											
4cyc											
0.0625	7.5									0.0049044	0.0046717
0.125	15		0.035898	0.015946		0.0082931		0.0058629	0.0034459	0.0025101	0.0021611
0.15	18										
0.175	21										
0.2	24										
0.225	27										
0.25	30		0.015699	0.0075197		0.005213		0.0027379	0.0025119	0.0022607	0.0019142
0.275	33										
0.3	36										
0.325	39										
0.35	42										
0.375	45										
0.4	48										
0.425	51										
0.45	54										
0.475	57										
0.5	60		0.005542	0.0054116		0.0037328		0.0027357	0.0021597	0.0020619	0.0019009
0.525	63										
0.55	66										
0.575	69										
0.6	72										
0.625	75										
0.65	78										
0.675	81										
0.7	84										
0.75	90		0.0046265	0.003493		0.0028821		0.0025134	0.0024644	0.0021717	0.0017595
0.8	96										
0.875	105										
0.9	108										
0.95	114										
1	120		0.0058992	0.0037937		0.0029		0.0024729	0.0021654	0.0021223	0.0017303

APPENDIX C

Subject-3

A	B	C	D	E	F	G	H	I	J	K	L
name				contrast		100%			SF=1.5 R=2.4		
proportion		2	3	4	5	6	7	8	10	12	16
0.03625											
2 cyc											
3 cyc											
4cyc											
0.0625	7.5										
0.125	15		0.030072	0.019303		0.013109		0.0054386	0.0041118	0.004249	0.0022438
0.15	18										
0.175	21										
0.2	24										
0.225	27										
0.25	30		0.012294	0.0077397		0.0031295		0.0023236	0.0021559	0.0017379	0.0018042
0.275	33										
0.3	36										
0.325	39										
0.35	42										
0.375	45										
0.4	48										
0.425	51										
0.45	54										
0.475	57										
0.5	60		0.0083796	0.0047642		0.002972		0.0016741	0.0018443	0.001574	0.0012725
0.525	63										
0.55	66										
0.575	69										
0.6	72										
0.625	75										
0.65	78										
0.675	81										
0.7	84										
0.75	90		0.0066678	0.0031825		0.0017821		0.0015157	0.0020289	0.0015366	0.0012881
0.8	96										
0.875	105										
0.9	108										
0.95	114										
1	120		0.0035306	0.0031433		0.0020445		0.0014519	0.0017771	0.0013076	0.0013967

Subject-4

A	B	C	D	E	F	G	H	I	J	K	L
name				contrast		100%			SF=1.5 R=2.4		
proportion		2	3	4	5	6	7	8	10	12	16
0.03625											
2 cyc											
3 cyc											
4cyc											
0.0625	7.5										0.0066558
0.125	15		0.034029	0.018977		0.011725		0.0047571	0.0049186	0.0029379	0.0025584
0.15	18										
0.175	21										
0.2	24										
0.225	27										
0.25	30		0.014777	0.0090209		0.0058366		0.0024829	0.0024114	0.0021685	0.0022941
0.275	33										
0.3	36										
0.325	39										
0.35	42										
0.375	45										
0.4	48										
0.425	51										
0.45	54										
0.475	57										
0.5	60		0.0055815	0.0045709		0.0042381		0.0022962	0.001998	0.0020548	0.0021101
0.525	63										
0.55	66										
0.575	69										
0.6	72										
0.625	75										
0.65	78										
0.675	81										
0.7	84										
0.75	90		0.0048262	0.0036229		0.0034311		0.0021712	0.0018235	0.0020476	0.0022418
0.8	96										
0.875	105										
0.9	108										
0.95	114										
1	120		0.0045347	0.0032618		0.0022847		0.002185	0.0019914	0.0018148	0.0022525

APPENDIX D

Subjec-5

A	B	C	D	E	F	G	H	I	J	K	L
name				contrast		100%			SF=1.5 R=2.4		
proportion		2	3	4	5	6	7	8	10	12	16
0.03625											
2 cyc											
3 cyc											
4cyc											
0.0625	7.5										
0.125	15		0.040889	0.031265				0.0052073		0.002371	
0.15	18										
0.175	21										
0.2	24										
0.225	27										
0.25	30		0.012301	0.0052467				0.0021627		0.0023937	
0.275	33										
0.3	36										
0.325	39										
0.35	42										
0.375	45										
0.4	48										
0.425	51										
0.45	54										
0.475	57										
0.5	60		0.0086304	0.0037557				0.002845		0.0021	
0.525	63										
0.55	66										
0.575	69										
0.6	72										
0.625	75										
0.65	78										
0.675	81										
0.7	84										
0.75	90		0.0059162	0.0037577				0.0025683		0.0018972	
0.8	96										
0.875	105										
0.9	108										
0.95	114										
1	120		0.0034704	0.004047				0.0024811		0.0017554	



APPENDIX E

Low-Contrast-Data

Subject-1

A	B	C	D	E	F	G	H	I	J	K	L	
name			contrast threshold			0.44284		5*th		3		
proportion		2	3	4	5	6	7	8	10	12	16	
0.125	15		0.048248	0.075596		0.049067		0.027517	0.016914	0.029357	0.015376	
0.15	18											
0.175	21											
0.2	24											
0.225	27											
0.25	30		0.016991	0.026135		0.022149		0.012148		0.012492	0.01365	
0.275	33											
0.3	36											
0.325	39											
0.35	42											
0.375	45							0.010275	0.0094961	0.013408	0.010637	
0.4	48											
0.425	51											
0.45	54											
0.475	57											
0.5	60		0.015993	0.020553		0.00883633		0.0064915	0.0061108	0.009843	0.009179	
0.525	63											
0.55	66											
0.575	69											
0.6	72											
0.625	75											
0.65	78											
0.675	81											
0.7	84											
0.75	90		0.0122	0.015929		0.01231		0.0059009	0.007568	0.011321	0.0098303	
0.8	96											
0.875	105											
0.9	108			0.0075741								
0.95	114											
1	120		0.0081936	0.013225		0.010341		0.007064	0.0086182	0.0081789	0.010485	

Subject-2

A	B	C	D	E	F	G	H	I	J	K	L	
name			contrast threshold			0.42585		5*th		3		
proportion		2	3	4	5	6	7	8	10	12	16	
0.125	15		0.077621	0.079351		0.026265		0.016769	0.016407	0.012303	0.01229	
0.15	18											
0.175	21											
0.2	24											
0.225	27											
0.25	30		0.056983	0.028448		0.017236		0.0070613	0.009581	0.00917	0.010022	
0.275	33											
0.3	36											
0.325	39											
0.35	42							0.0079128	0.0094645	0.0076135		
0.375	45											
0.4	48											
0.425	51											
0.45	54											
0.475	57											
0.5	60		0.027813	0.024801		0.011651		0.0087884	0.0089035	0.0058702	0.0092253	
0.525	63											
0.55	66											
0.575	69											
0.6	72											
0.625	75											
0.65	78											
0.675	81											
0.7	84											
0.75	90		0.022538	0.01651		0.010777		0.0061115	0.0087906	0.0090486	0.0084211	
0.8	96									0.0084085		
0.875	105											
0.9	108			0.016598		0.0089673						
0.95	114											
1	120		0.0093089	0.012408		0.0071429		0.007642	0.006821	0.0085961	0.0087675	

APPENDIX F

Subject-3

name			contrast threshold		1.2547	5*th	6.273				
proportion		2	3	4	5	6	7	8	10	12	16
0.125	15		0.077017	0.038421		0.024856		0.012924	0.011368	0.0069388	0.0066856
0.15	18									0.005875	
0.175	21										
0.2	24							0.0060895		0.0053116	0.004371
0.225	27										
0.25	30		0.019969	0.014357		0.011989		0.0038855	0.0071052	0.0046336	0.0055086
0.275	33										
0.3	36										
0.325	39										
0.35	42										
0.375	45			0.010499		0.0074203			0.0062886	0.0050247	
0.4	48			0.0089635							
0.425	51										
0.45	54										
0.475	57										
0.5	60		0.011626	0.011574		0.0080336		0.0047097	0.0071635	0.0042692	0.0041597
0.525	63										
0.55	66										
0.575	69										
0.6	72										
0.625	75			0.006206		0.0077364					
0.65	78										
0.675	81										
0.7	84										
0.75	90		0.0081505	0.0086287		0.0067435		0.0044124	0.0059016	0.0043495	0.0060508
0.8	96										
0.875	105										
0.9	108										
0.95	114										
1	120		0.0055708	0.004		0.0054983		0.0034	0.0053063	0.0046632	0.0036909

Subject-4

name			contrast threshold		0.34978	5*th	2		4		
proportion		2	3	4	5	6	7	8	10	12	16
0.125	15			0.074022		0.035896		0.028702	0.015861	0.01487	0.018072
0.15	18										
0.175	21										
0.2	24							0.013829	0.010264	0.012625	0.010572
0.225	27										
0.25	30		0.057565	0.02762		0.015466		0.0079806	0.00786269	0.0068236	0.011952
0.275	33										
0.3	36					0.011884					
0.325	39										
0.35	42										
0.375	45			0.015921		0.010764		0.0069534	0.0094086	0.0086425	0.010926
0.4	48										
0.425	51										
0.45	54										
0.475	57										
0.5	60		0.017652	0.011808		0.0099451		0.0060149	0.0061883	0.0082086	0.0073533
0.525	63										
0.55	66										
0.575	69										
0.6	72								0.0068707		
0.625	75										
0.65	78										
0.675	81										
0.7	84										
0.75	90		0.012888	0.010287		0.0081593		0.0086173	0.009942	0.0065991	0.011532
0.8	96										
0.875	105		0.0098589	0.008085							
0.9	108										
0.95	114										
1	120		0.0065854	0.0078128		0.007593		0.0055415	0.004032	0.005309	0.010759

APPENDIX G

Subject-5

A	B	C	D	E	F	G	H	I	J	K	L	
name			contrast threshold			0.41327		5*th	2.5			
proportion		2	3	4	5	6	7	8	10	12	16	
0.125	15		0.089223	0.058423		0.036469		0.029427	0.012241	0.012683	0.015573	
0.15	18											
0.175	21											
0.2	24							0.012464				
0.225	27											
0.25	30		0.036183	0.022609		0.014312		0.0096316	0.0088068	0.01024	0.010728	
0.275	33											
0.3	36											
0.325	39											
0.35	42											
0.375	45			0.019605		0.015037		0.0091915	0.0072629			
0.4	48											
0.425	51											
0.45	54			0.017202								
0.475	57											
0.5	60		0.018737	0.012301		0.010472		0.0092569	0.010142	0.0099229	0.010867	
0.525	63											
0.55	66											
0.575	69											
0.6	72			0.013575								
0.625	75											
0.65	78											
0.675	81											
0.7	84											
0.75	90		0.012922	0.010491		0.0092075		0.010215	0.011241	0.0093305	0.011641	
0.8	96											
0.875	105											
0.9	108											
0.95	114											
1	120		0.011802	0.0089516		0.0072213		0.00905	0.0086553	0.0087103	0.0089036	

Subject-6

A	B	C	D	E	F	G	H	I	J	K	L	
name			contrast threshold			0.37924		5*th	2			
proportion		2	3	4	5	6	7	8	10	12	16	
0.125	15		0.075045	0.070224		0.029055		0.020165	0.013217	0.021766	0.013296	
0.15	18											
0.175	21											
0.2	24										0.012817	
0.225	27											
0.25	30		0.027606	0.026151		0.018844		0.01289	0.010516	0.0072806	0.0097964	
0.275	33											
0.3	36											
0.325	39							0.0067575				
0.35	42											
0.375	45			0.019961				0.0079153		0.00758	0.009495	
0.4	48											
0.425	51											
0.45	54											
0.475	57											
0.5	60		0.015956	0.017697		0.014103		0.0070891	0.0077478	0.0096813	0.010544	
0.525	63											
0.55	66											
0.575	69											
0.6	72											
0.625	75			0.014794								
0.65	78											
0.675	81			0.013563								
0.7	84											
0.75	90		0.010045	0.012602		0.011088		0.0067914	0.0092135	0.010318	0.011157	
0.8	96											
0.875	105											
0.9	108					0.0096125						
0.95	114											
1	120		0.0099494	0.011508		0.007192		0.007208	0.0082863	0.0080044	0.0085164	

APPENDIX H

Subject-7

A	B	C	D	E	F	G	H	I	J	K	L	
name			contrast threshold			0.39572		5*th	2.5			
proportion		2	3	4	5	6	7	8	10	12	16	
0.125	15		0.0939	0.036939		0.026893		0.022223	0.020346	0.015831	0.014057	
0.15	18											
0.175	21											
0.2	24											
0.225	27											
0.25	30		0.035185	0.018026		0.011099		0.0099267	0.0087609	0.0095107	0.010102	
0.275	33											
0.3	36											
0.325	39											
0.35	42											
0.375	45			0.01667		0.0123				0.010077		
0.4	48											
0.425	51											
0.45	54											
0.475	57											
0.5	60		0.01694	0.016754		0.010496		0.0091342	0.0099969	0.0080329	0.0097995	
0.525	63											
0.55	66											
0.575	69											
0.6	72											
0.625	75											
0.65	78					0.010472						
0.675	81											
0.7	84											
0.75	90		0.011351	0.0132		0.0094683		0.0095334	0.0090418	0.010506	0.01043	
0.8	96											
0.875	105											
0.9	108			0.010462								
0.95	114											
1	120		0.01028	0.0092738		0.0082825		0.0085613	0.0087402	0.0083661	0.010164	

Subject-8

A	B	C	D	E	F	G	H	I	J	K	L	
name			contrast threshold			0.63646		5*th	3.18			
proportion		2	3	4	5	6	7	8	10	12	16	
0.125	15		0.073964	0.050663		0.016632		0.014732	0.013685	0.012485	0.013635	
0.15	18											
0.175	21											
0.2	24											
0.225	27											
0.25	30		0.029402	0.024338		0.012301		0.0078281	0.0083539	0.0084843	0.0093514	
0.275	33											
0.3	36											
0.325	39											
0.35	42											
0.375	45							0.0055513	0.0065195	0.0056556	0.0083546	
0.4	48											
0.425	51											
0.45	54											
0.475	57											
0.5	60		0.01167	0.016318		0.011251		0.0058994	0.0061358	0.0054459	0.0079652	
0.525	63											
0.55	66											
0.575	69											
0.6	72											
0.625	75					0.0089917						
0.65	78											
0.675	81											
0.7	84											
0.75	90		0.014321	0.010692		0.0054116		0.0049195	0.0081342	0.0068017	0.0085878	
0.8	96											
0.875	105											
0.9	108			0.0091036								
0.95	114											
1	120		0.010945	0.0055986		0.0065827		0.0053867	0.006915	0.0053562	0.0075759	

APPENDIX I

Closed-Circle-Data

Subject-1

A	B	C	D	E	F
name		contrast	100%	SF=1.5 R=2.4	
proportion		c0	c4	c8	c10
0.03625					
2 cyc					
3 cyc					
4cyc					
0.0625	7.5				
0.125	15			0.0060458	
0.15	18				
0.175	21				
0.2	24				
0.225	27				
0.25	30		0.0084532	0.0036798	
0.275	33				
0.3	36				
0.325	39				
0.35	42				
0.375	45				
0.4	48				
0.425	51				
0.45	54				
0.475	57				
0.5	60		0.0054719	0.0023045	
0.525	63				
0.55	66				
0.575	69				
0.6	72				
0.625	75				
0.65	78				
0.675	81				
0.7	84				
0.75	90		0.0040616	0.0020575	
0.8	96				
0.875	105				
0.9	108				
0.95	114				
1	120		0.003733	0.0017	

APPENDIX J

Subject-2

A	B	C	D	E	F
name		contrast	100%	SF=1.5 R=2.4	
proportion		c0	c4	c8	c10
0.03625					
2 cyc					
3 cyc					
4cyc					
0.0625	7.5				
0.125	15			0.0050141	
0.15	18				
0.175	21				
0.2	24				
0.225	27				
0.25	30		0.0079982	0.0045144	
0.275	33				
0.3	36				
0.325	39				
0.35	42				
0.375	45				
0.4	48				
0.425	51				
0.45	54				
0.475	57				
0.5	60		0.0070748	0.003662	
0.525	63				
0.55	66				
0.575	69				
0.6	72				
0.625	75				
0.65	78				
0.675	81				
0.7	84				
0.75	90		0.0053912	0.0031123	
0.8	96				
0.875	105				
0.9	108				
0.95	114				
1	120		0.0032391	0.0028839	



APPENDIX K

Subject-3

A	B	C	D	E	F
name		contrast	100%	SF=1.5 R=2.4	
proportion		c0	c4	c8	c10
0.03625					
2 cyc					
3 cyc					
4cyc					
0.0625	7.5				
0.125	15			0.0047852	
0.15	18				
0.175	21				
0.2	24				
0.225	27				
0.25	30		0.0095731	0.0032804	
0.275	33				
0.3	36				
0.325	39				
0.35	42				
0.375	45				
0.4	48				
0.425	51				
0.45	54				
0.475	57				
0.5	60		0.005317	0.0023986	
0.525	63				
0.55	66				
0.575	69				
0.6	72				
0.625	75				
0.65	78				
0.675	81				
0.7	84				
0.75	90		0.0032741	0.0017214	
0.8	96				
0.875	105				
0.9	108				
0.95	114				
1	120		0.0035267	0.0012835	

Subject-4

A	B	C	D	E	F
name		contrast	100%	SF=1.5 R=2.4	
proportion		c0	c4	c8	c10
0.03625					
2 cyc					
3 cyc					
4cyc					
0.0625	7.5				
0.125	15			0.007378	
0.15	18				
0.175	21				
0.2	24				
0.225	27				
0.25	30		0.0095542	0.0052438	
0.275	33				
0.3	36				
0.325	39				
0.35	42				
0.375	45				
0.4	48				
0.425	51				
0.45	54				
0.475	57				
0.5	60		0.0060426	0.0024554	
0.525	63				
0.55	66				
0.575	69				
0.6	72				
0.625	75				
0.65	78				
0.675	81				
0.7	84				
0.75	90		0.0040235	0.0021225	
0.8	96				
0.875	105				
0.9	108				
0.95	114				
1	120		0.0036338	0.0020427	

APPENDIX L

Glare-Experiment-Data

Subject-1

High	RF=4	RF_100_cstH_glare	0.0169
Luminance		RF_100_cstH_noglare	0.0063
		RF_100_cstL_noglare	0.0099
		RF_75_cstL_noglare	0.0161
		RF_50_cstL_noglare	0.0244
	RF=3	RF_100_cstH_glare	0.022
		RF_100_cstH_noglare	0.0068
		RF_100_cstL_noglare	0.0135
		RF_75_cstL_noglare	0.0188
		RF_50_cstL_noglare	0.0238
Low	RF=4	RF_100_cstH_glare	0.0218
Luminance		RF_100_cstH_noglare	0.0086
		RF_100_cstL_noglare	0.0141
		RF_75_cstL_noglare	0.0243
		RF_50_cstL_noglare	0.031
	RF=3	RF_100_cstH_glare	0.1463
		RF_100_cstH_noglare	0.0111
		RF_100_cstL_noglare	0.0375
		RF_75_cstL_noglare	0.0623
		RF_50_cstL_noglare	0.0669

Subject-2

High	RF=4	RF_100_cstH_glare	0.0123
Luminance		RF_100_cstH_noglare	0.0053
		RF_100_cstL_noglare	0.0099
		RF_75_cstL_noglare	0.0162
		RF_50_cstL_noglare	0.0301
	RF=3	RF_100_cstH_glare	0.0265
		RF_100_cstH_noglare	0.0078
		RF_100_cstL_noglare	0.0158
		RF_75_cstL_noglare	0.0187
		RF_50_cstL_noglare	0.0299
Low	RF=4	RF_100_cstH_glare	0.0267
Luminance		RF_100_cstH_noglare	0.0062
		RF_100_cstL_noglare	0.0128
		RF_75_cstL_noglare	0.0187
		RF_50_cstL_noglare	0.0276
	RF=3	RF_100_cstH_glare	0.1145
		RF_100_cstH_noglare	0.0091
		RF_100_cstL_noglare	0.0529
		RF_75_cstL_noglare	0.0566
		RF_50_cstL_noglare	0.0652



APPENDIX M

Subject-3

High	RF=4	RF_100_cstH_glare	0.0125
Luminance		RF_100_cstH_noglare	0.0072
		RF_100_cstL_noglare	0.0082
		RF_75_cstL_noglare	0.0121
		RF_50_cstL_noglare	0.0216
	RF=3	RF_100_cstH_glare	0.0285
		RF_100_cstH_noglare	0.0073
		RF_100_cstL_noglare	0.0123
		RF_75_cstL_noglare	0.0234
		RF_50_cstL_noglare	0.0304
Low	RF=4	RF_100_cstH_glare	0.0292
Luminance		RF_100_cstH_noglare	0.0082
		RF_100_cstL_noglare	0.0145
		RF_75_cstL_noglare	0.0131
		RF_50_cstL_noglare	0.0329
	RF=3	RF_100_cstH_glare	0.1229
		RF_100_cstH_noglare	0.0105
		RF_100_cstL_noglare	0.0512
		RF_75_cstL_noglare	0.0594
		RF_50_cstL_noglare	0.0631

APPENDIX N

Subject-4

High	RF=4	RF_100_cstH_glare	0.0131
Luminance		RF_100_cstH_noglare	0.0045
		RF_100_cstL_noglare	0.0094
		RF_75_cstL_noglare	0.014
		RF_50_cstL_noglare	0.0258
	RF=3	RF_100_cstH_glare	0.0307
		RF_100_cstH_noglare	0.0118
		RF_100_cstL_noglare	0.011
		RF_75_cstL_noglare	0.0202
		RF_50_cstL_noglare	0.0261
Low	RF=4	RF_100_cstH_glare	0.0365
Luminance		RF_100_cstH_noglare	0.0064
		RF_100_cstL_noglare	0.0126
		RF_75_cstL_noglare	0.0169
		RF_50_cstL_noglare	0.0191
	RF=3	RF_100_cstH_glare	0.0857
		RF_100_cstH_noglare	0.0066
		RF_100_cstL_noglare	0.0494
		RF_75_cstL_noglare	0.0569
		RF_50_cstL_noglare	0.0703

APPENDIX O

Subject-5

High	RF=4	RF_100_cstH_glare	0.0083
Luminance		RF_100_cstH_noglare	0.0059
		RF_100_cstL_noglare	0.0092
		RF_75_cstL_noglare	0.0113
		RF_50_cstL_noglare	0.0236
	RF=3	RF_100_cstH_glare	0.0324
		RF_100_cstH_noglare	0.0079
		RF_100_cstL_noglare	0.0109
		RF_75_cstL_noglare	0.0199
		RF_50_cstL_noglare	0.0279
Low	RF=4	RF_100_cstH_glare	0.0237
Luminance		RF_100_cstH_noglare	0.0098
		RF_100_cstL_noglare	0.0149
		RF_75_cstL_noglare	0.0232
		RF_50_cstL_noglare	0.0263
	RF=3	RF_100_cstH_glare	0.0947
		RF_100_cstH_noglare	0.009
		RF_100_cstL_noglare	0.0393
		RF_75_cstL_noglare	0.0437
		RF_50_cstL_noglare	0.0534

Subject-6

High	RF=4	RF_100_cstH_glare	0.0181
Luminance		RF_100_cstH_noglare	0.0058
		RF_100_cstL_noglare	0.0103
		RF_75_cstL_noglare	0.0116
		RF_50_cstL_noglare	0.0285
	RF=3	RF_100_cstH_glare	0.0267
		RF_100_cstH_noglare	0.0097
		RF_100_cstL_noglare	0.0149
		RF_75_cstL_noglare	0.0239
		RF_50_cstL_noglare	0.0223
Low	RF=4	RF_100_cstH_glare	0.0271
Luminance		RF_100_cstH_noglare	0.0076
		RF_100_cstL_noglare	0.0154
		RF_75_cstL_noglare	0.0162
		RF_50_cstL_noglare	0.0222
	RF=3	RF_100_cstH_glare	0.0977
		RF_100_cstH_noglare	0.0083
		RF_100_cstL_noglare	0.0575
		RF_75_cstL_noglare	0.0567
		RF_50_cstL_noglare	0.0874